Atherosclerosis 390 (2024) 117450

Contents lists available at ScienceDirect

Atherosclerosis

journal homepage: www.elsevier.com/locate/atherosclerosis

Metabolic reprogramming of immune cells by mitochondrial division inhibitor-1 to prevent post-vascular injury neointimal hyperplasia

Gustavo E. Crespo-Avilan [a,b,c], Sauri Hernandez-Resendiz [b,c], Chrishan J. Ramachandra [b,c], Victor Ungureanu [d], Ying-Hsi Lin [b,c], Shengjie Lu [b,c], Jürgen Bernhagen [f,g,h], Omar El Bounkari [f], Klaus T. Preissner [a,i], Elisa A. Liehn [c,d,e,1,**], Derek J. Hausenloy [b,c,j,k,1,*]

[a] Department of Biochemistry, Medical Faculty, Justus Liebig-University, Giessen, Germany
[b] Cardiovascular and Metabolic Disorders Program, Duke-National University of Singapore Medical School, Singapore
[c] National Heart Research Institute Singapore, National Heart Centre Singapore, Singapore
[d] National Institute of Pathology, "Victor Babes", Bucharest, Romania
[e] Institute for Molecular Medicine, University of South Denmark, Odense, Denmark
[f] Division of Vascular Biology, Institute for Stroke and Dementia Research, University Hospital, Ludwig-Maximilians-University, Munich, Germany
[g] Munich Cluster for Systems Neurology (SyNergy), Munich, Germany
[h] Munich Heart Alliance, Munich, Germany
[i] Kerckhoff-Heart-Research-Institute, Department of Cardiology, Medical School, Justus-Liebig-University, Giessen, Germany
[j] The Hatter Cardiovascular Institute, University College London, London, WC1E 6BT, UK
[k] Yong Loo Lin School of Medicine, National University Singapore, Singapore

ARTICLE INFO

Keywords:
Mdivi-1
Vascular restenosis
Neointimal hyperplasia
Monocytes/macrophages
Inflammation
Mitochondrial fission

ABSTRACT

Background and aims: New treatments are needed to prevent neointimal hyperplasia that contributes to post-angioplasty and stent restenosis in patients with coronary artery disease (CAD) and peripheral arterial disease (PAD). We investigated whether modulating mitochondrial function using mitochondrial division inhibitor-1 (Mdivi-1) could reduce post-vascular injury neointimal hyperplasia by metabolic reprogramming of macrophages from a pro-inflammatory to anti-inflammatory phenotype.

Methods and Results: In vivo Mdivi-1 treatment of *Apoe*$^{-/-}$ mice fed a high-fat diet and subjected to carotid-wire injury decreased neointimal hyperplasia by 68%, reduced numbers of plaque vascular smooth muscle cells and pro-inflammatory M1-like macrophages, and decreased plaque inflammation, endothelial activation, and apoptosis, when compared to control. Mdivi-1 treatment of human THP-1 macrophages shifted polarization from a pro-inflammatory M1-like to an anti-inflammatory M2-like phenotype, reduced monocyte chemotaxis and migration to CCL2 and macrophage colony stimulating factor (M-CSF) and decreased secretion of pro-inflammatory mediators. Finally, treatment of pro-inflammatory M1-type-macrophages with Mdivi-1 metabolically reprogrammed them to an anti-inflammatory M2-like phenotype by inhibiting oxidative phosphorylation and attenuating the increase in succinate levels and correcting the decreased levels of arginine and citrulline.

Conclusions: We report that treatment with Mdivi-1 inhibits post-vascular injury neointimal hyperplasia by metabolic reprogramming macrophages towards an anti-inflammatory phenotype thereby highlighting the therapeutic potential of Mdivi-1 for preventing neointimal hyperplasia and restenosis following angioplasty and stenting in CAD and PAD patients.

1. Introduction

Atherosclerotic coronary arterial disease (CAD) and peripheral arterial disease (PAD) are among the leading causes of death and disability worldwide [1]. Despite intensive research, there are no effective treatments for preventing the onset or progression of

* Corresponding authorInstitute for Molecular Medicine, University of Southern Denmark, Odense, Denmark,
** Corresponding authorCardiovascular & Metabolic Disorders Program Duke-National University of Singapore Medical School, Singapore.
E-mail addresses: liehn@health.sdu.dk (E.A. Liehn), derek.hausenloy@duke-nus.edu.sg (D.J. Hausenloy).
[1] These authors contributed equally to the manuscript.

https://doi.org/10.1016/j.atherosclerosis.2024.117450
Received 11 October 2022; Received in revised form 23 December 2023; Accepted 9 January 2024
Available online 14 January 2024

atherosclerosis in these patients. Revascularization by angioplasty and stenting remain the main stay of treatment for many patients with CAD and PAD, but this procedure is associated with a significant risk of restenosis, the results of which are repeated episodes of revascularization and increased likelihood of complications. The key contributor to post-angioplasty restenosis is tunica neointima hyperplasia and infiltration of inflammatory cells [2,3]. As such, new treatments are needed to inhibit neointimal hyperplasia to prevent post-angioplasty restenosis in CAD and PAD patients to improve health outcomes in these patients.

Mitochondria regulate ROS generation, calcium handling, and ATP synthesis [4], processes implicated in cell migration, proliferation [5], and macrophage polarization during inflammation in the setting of CAD [6]. Metabolic adaptations have been shown to contribute to the polarization of macrophages into different macrophage phenotypes. Recent next-generation and single-cell RNA sequencing data have underscored the plasticity of macrophages and revealed a previously unanticipated variety of macrophage identities [7,8]. Still, the classical categorization into M1-like proinflammatory or M2-like anti-inflammatory phenotypes holds utility and has been demonstrated to be linked to metabolic adaptions of these cells. These divergent metabolic profiles play a pivotal role in dictating macrophage function within the atherosclerotic plaque microenvironment, often dominated by the proinflammatory M1-like state, which significantly contributes to plaque formation and progression [9]. The growing field of immunometabolism has emerged as a promising frontier for manipulating the immune response, particularly by targeting mitochondrial metabolism.

Notably, M1-like macrophages are characterized by augmented glycolysis and pentose phosphate pathway activity, leading to increased production of proinflammatory cytokines, and the accumulation of metabolites such as succinate, which can potentiate inflammation through HIF1α regulation. Conversely, M2-like macrophages favor mitochondrial oxidative phosphorylation and fatty acid oxidation, aligning with their anti-inflammatory and tissue repair functions [10]. This intricate interplay between macrophage polarization, mitochondria metabolism, and the dynamic plaque microenvironment underscores the importance of modulating immunometabolism to modulate the immune response [11]. In this context, mitochondrial division inhibitor-1 (Mdivi-1), known initially for its ability to regulate mitochondrial fission by inhibiting the dynamin-related protein 1 (Drp1), a GTPase that regulates mitochondrial fission in different cell types, has exhibited beneficial effects in ameliorating cardiovascular diseases [12]. However, Mdivi-1 is demonstrated to not be a specific human Drp1 inhibitor, but also targets mitochondrial Complex I, mediating reactive oxygen species (ROS) production [13]. Thus, Mdivi-1 can serve as a therapeutic candidate to modulate mitochondrial metabolism, offering innovative avenues to influence macrophage polarization and temper the inflammatory processes associated with atherosclerosis.

Therefore, we hypothesized that modulating mitochondrial function to target inflammation can impact on the formation and progression of atheroma following mechanical vascular injury. In this regard, in this study, we tested the influence of Mdivi-1 [14,15] on neointimal hyperplasia and plaque inflammation and progression in a carotid wire-injury mouse model.

2. Materials and methods

2.1. Carotid artery wire-induced vascular injury mouse model

All experiments were approved by the Biomedical Sciences Institute Singapore Institutional Animal Care Committee and were undertaken in compliance with the Recommendation of the American Heart Association on Design, Execution, and Reporting of Animal Atherosclerosis Studies [16]. Male 10- to 12-week-old *Apoe*$^{-/-}$ mice (C57BL/6J background) were obtained from Charles River Laboratory (Italy) and maintained on a 12h dark-light cycle. Mice were placed on a high-fat diet (21% fat, 0.15% cholesterol: Altromin) for three weeks, starting one week before and continued until two weeks post-vascular injury. The wire-induced injury procedure was performed as previously described [17]. Briefly, mice were anesthetized (100 mg/kg ketamine hydrochloride/10 mg/kg xylazine intraperitoneal [IP]) and subjected to endothelial denudation of the left common carotid artery by inserting a 0.36 mm guidewire through a transverse arteriotomy of the external carotid artery. Prior to surgery and up to three days post-surgery, analgesia was administered via subcutaneous injection of Buprenorphine (0.05–0.1 mg/kg). *Apoe*$^{-/-}$ mice continuously received Mdivi-1 (1.2 mg/kg/day) or vehicle during the experiment using Alzet osmotic mini-pumps, subcutaneously implanted 1 day before surgery.

2.2. Histology and immunofluorescence

Two weeks after the vascular injury procedure, mice were anesthetized (100 mg/kg ketamine hydrochloride/10 mg/kg xylazine IP) and perfused *in situ* with 4% paraformaldehyde. The injured carotid arteries were excised, fixed in 4% para-formaldehyde, dehydrated, and embedded in paraffin. Arteries were subsequently cut in 5 μm serial transverse sections (9 sections/mouse, 50 μm apart) collected within a distance of up to 320 μm from the bifurcation, stained using Elastica-van Gieson, and the injury-related plaque areas (lumen, neointima and media) were measured by planimetry using Diskus Software (Hilgers) as previously described [18]. For each mouse, data from the nine sections were averaged to represent lesion formation along this standardized distance. Adjacent sections were used to assess cellular plaque content. Total cell quantification was performed by nuclei staining using DAPI, whereas visualization of endothelial cells, macrophages, and smooth muscle cells was achieved by immunofluorescence staining for CD31 (cluster of differentiation 31; M-20; Santa Cruz Biotechnology), MAC-2 (Galectin-3; M3/38; Cedarlane), or SMA (smooth muscle actin; 1A4; Dako), respectively, followed by secondary antibody staining using fluorescein isothiocyanate (FITC)–conjugated or Cy3-conjugated antibodies (Jackson ImmunoResearch) as previously described [19]. Plaque-related inflammatory markers were also visualized using immunofluorescence staining of TNF-α and ICAM-1. The polarization of macro-phages in the plaque was identified by double staining of MAC-2 and Myeloperoxidase (MPO) (Neomarkers, ThermoFisher Scientific). Further, we have used Phyton to develop a new software program for automated segmentation of vascular structures, automatic calculations of the volumes of different vascular structures, as well as automatic 3D reconstruction of the injured vessels (500 μm starting with the bifurcation) using 10 sections, 50 μm apart.

2.3. Cell culture, differentiation and treatment

The THP-1 cell line was obtained from ATCC and maintained at 2.5x10^5 cells/ml in RPMI 1640 medium supplemented with 10% FBS and 1% L-glutamine at 37 °C and 5% CO_2. THP-1 cells (1x10^6 cells/mL) were seeded in a six-well plate (Costar) and differentiated to macrophages as described [20]. Briefly, cells were treated with 10 ng/mL phorbol 12-myristate 13-acetate (PMA, Sigma-Aldrich) for 48 h followed by a resting period incubating the cells in fresh RPMI 1640 (10% FBS, 1% L-glutamine) for a further 24h (PMA-free). Cells were treated with Mdivi-1 at a final concentration of 50 μM (TOCRIS) dissolved in DMSO (SIGMA). Control groups were treated with DMSO using a final concentration of 0.1%. To induce proinflammatory (M1-like) or anti-inflammatory profile (M2-like), cells were treated with a mix of 100 ng/mL of LPS (LPS-EB Ultrapure - InvivoGen) and 20 ng/mL of IFN-y (Miltenyi Biotec) or 20 ng/mL of IL-4 (Miltenyi Biotec), respectively. THP-1-derived macrophages were detached by trypLE Express (Gibco) according to the manufacturer's instructions. At the end of the study, supernatants and cell pellets were collected and stored at −80 °C for further analysis. Cell viability and cytotoxicity were assessed by trypan blue exclusion test and cytotoxicity detection kit (LDH; Roche), respectively.

2.4. Cell culture of murine bone marrow-derived macrophages (BMDM)

BMDMs were derived from the femurs of male C57BL/6J mice aged 10–12 weeks (Jackson Laboratory). The process involved isolating bone marrow cells and culturing them as previously described [21]. In essence, these cells were incubated in Dulbecco's Modified Eagle Media (DMEM, Gibco) complemented with 10% heat-inactivated fetal bovine serum (FBS) sourced from Life Technologies, 1% penicillin/streptomycin, 1% glutamine, and 20% L929 cell supernatant, which served as the M-CSF provider. On the 7th day of culture, the cells underwent a wash and were re-plated in DMEM media without L929 supernatant, with a cell density of 200,000 cells per well in a 96-well polystyrene Seahorse plate. After a 24h period, macrophages were subjected to a 6h stimulation using the same concentrations of stimulating agents, mirroring those used for human THP-1 cells, to induce M1-like and M2-like polarization. This was performed both in the presence or absence of Mdivi-1.

2.5. Isolation of human peripheral blood mononuclear cells

Peripheral blood mononuclear cells were isolated as previously described [22]. Briefly, peripheral blood was collected and mixed with an equal volume of phosphate-buffered saline (PBS); peripheral blood mononuclear cells were isolated by density gradient centrifugation using Ficoll-Paque Plus (GE Healthcare, Germany). After centrifugation, cells in the interphase were carefully collected and subsequently washed with pre-warmed PBS (Invitrogen). The pellet was then resuspended in RPMI 1640 medium (Invitrogen) supplemented with 10% FCS, 1% penicillin/streptomycin, 2 mM L-glutamine and 1% non-essential amino acids (Sigma Aldrich, Germany). Cells were maintained at 37 °C in a humidified atmosphere of 5% CO_2. Primary human monocytes were then purified by negative depletion using the Monocytes Isolation Kit II from Miltenyi Biotec (Bergisch Gladbach, Germany) according to the manufacturer's protocol. The purity of isolated monocytes was analysed by flow cytometry (FACS) using an anti-CD14 (Miltenyi Biotec). The mentioned isolation protocol was approved by the local ethics committee and carried out in accordance with the guidelines of the National Heart Centre of Singapore (CIRB ref 2018/2497) and LMU Munich University Hospital.

2.6. Cell migration assays

The migratory behavior of isolated human peripheral blood monocytes in response to CCL2 was assessed using 3D chemotaxis μ-Slide (Ibidi GmbH, Munich, Germany) according to the manufacturer's protocol and previously established procedures [23–25]. Briefly, freshly isolated monocytes ($4.0x10^6$) were seeded in a gel containing 1 mg/ml rat tail collagen type I and 1x DMEM. The collagen gel-containing cell suspension was incubated at 37 °C for 30 min for polymerization and was subsequently subjected to a gradient of MCP-1/CCL2 (100 ng/ml) in the presence or absence of Mdivi-1 (10 μM or 50 μM). Cell motility was monitored by performing time-lapse imaging every 2 min at 37 °C for 2h using a Leica DMi8 M Microscope (Leica, Germany). Images were imported as stacks to ImageJ software and were analysed with manual tracking using the chemotaxis and migration tools from Ibidi GmbH (Munich, Germany). Transwell chemotaxis assays were performed using a 24-well Transwell plate (6.5 mm diameter, 8 μm pore size, Costar) as described [26] with some modifications. Briefly, the bottom chamber of the Transwell was filled with RPMI 1640 medium 0.5% (vol/vol) FBS medium containing human macrophage colony-stimulating factor (Miltenyi Biotec) as a chemoattractant (20 ng/mL). Thereafter, $2.5x10^5$ THP-1 cells were placed on the top of the insert-filter in RPMI 1640 medium containing 0.5% FBS. After 6h of incubation at 37 °C, the bottom chamber was harvested, and the viable transmigrated cells were counted in a Countess II FL Automated Cell Counter (Life Technologies) as previously described [20]. For the experiments of chemotaxis inhibition, cells were seeded on the top of the filter in the mentioned media with 50 μM Mdivi-1 (TOCRIS) dissolved in DMSO (SIGMA). For the control, the same final concentration of DMSO (0.5%) was used.

2.7. RNA isolation and real-time PCR analysis

Total RNA was prepared from cell lysates using Qiagen RNeasy Mini kit, according to the manufacturer's instructions and immediately subjected to DNase digestion process using RNase-free DNase I (Thermo Scientific) including the application of Thermo Scientific RiboLock RNase Inhibitor, following the manufacturer's instructions. Synthesis of cDNA was performed using iScript™ cDNA Synthesis Kit (BIO-RAD) following the manufactured protocol. For each cDNA synthesis, 1 μg of total RNA was used. Complementary DNA was diluted to a final concentration of 1 ng/μL and stored at −20 °C prior to PCR analyses. Real-time PCR analysis was performed using specific primer pairs purchased from Sigma-Aldrich, on an Applied Biosystems Viia 7 instrument, with PrecisionFAST™ 2X qPCR Mastermix (PrimerDesing). PCR runs included a 2 min pre-incubation at 95 °C to allow heat activation of polymerase, followed by 40 cycles of a three-step PCR consisting of a denaturing phase at 95 °C for 5 s and an annealing phase at 64 °C for 5 s and an extension phase at 72 °C for 10 s. After completion of PCR, a melting curve was recorded, and the expression of target genes was normalized to the housekeeping gene (beta-actin). RT-PCR data were analysed using the comparative Ct method [27].

2.8. Western blot analysis

Cell pellets from THP-1-Monocytes were lysed with RIPA buffer (Thermo Fisher Scientific) and protein concentration was quantified using the BCA protein assay kit (Thermo Fisher Scientific). Equal amounts of solubilised proteins were electrophoretically resolved by 10% SDS-PAGE and then transferred to a PVDF membrane using the Trans-Blot Turbo system (Bio-Rad). The membranes were blocked in 5% (w/v) of blotting-grade blocker (Bio-Rad) and subsequently incubated overnight at 4 °C with the following monoclonal antibodies (1:1000; Cell Signalling): anti-phospho-Drp1 (Ser616), anti-phosphor-DRP1 (Ser637) or anti-Drp1 (D6C7). The monoclonal antibody anti-GAPDH (1:1000; Cell Signalling) was used as a loading control. After washing, membranes were incubated for 2h with horseradish peroxidase (HRP)-conjugated secondary antibodies (1:2000; Cell Signalling Technology). Antibody binding was detected using a chemiluminescence reaction (Cell Signalling Technology) with the Bio-Rad Chemi-Doc instrument and bands-optical density analysis was performed using ImageJ.

2.9. Confocal fluorescence microscopy and image analysis

Control and stimulated THP-1 monocytes were seeded on poly-D-lysine coated glass-bottom dishes (Thermo) and fixed with 4% PFA, permeabilised with 0.1% Triton X-100, blocked with 5% BSA, and stained with COX-IV antibody (1:250 dilution; Cell Signaling Technology #4850) overnight at 4 °C. The following day, cells were washed and stained with Alexa Fluor 488–conjugated secondary antibodies (1:400 dilution Life Technologies) for 1h at room temperature, and counterstained with DAPI. Stained cells were examined under Zeiss LSM710 confocal microscope (Carl Zeiss). For mitochondria morphometric assessment, blinded analysis was performed by two independent researchers using an ImageJ workflow as previously described [28].

2.10. Measurement of cellular respiration (MitoStress assay)

The XF96 extracellular flux analyser (Seahorse Biosciences, North Billerica, MA) was used to determine the bioenergetic profile of THP-1 cells and BMDM. Briefly, THP-1 monocytes were plated on poly-D-lysine-coated plates and THP-1 macrophages were differentiated on the same plate type (96-well polystyrene Seahorse plate) at 200,000 cells per well

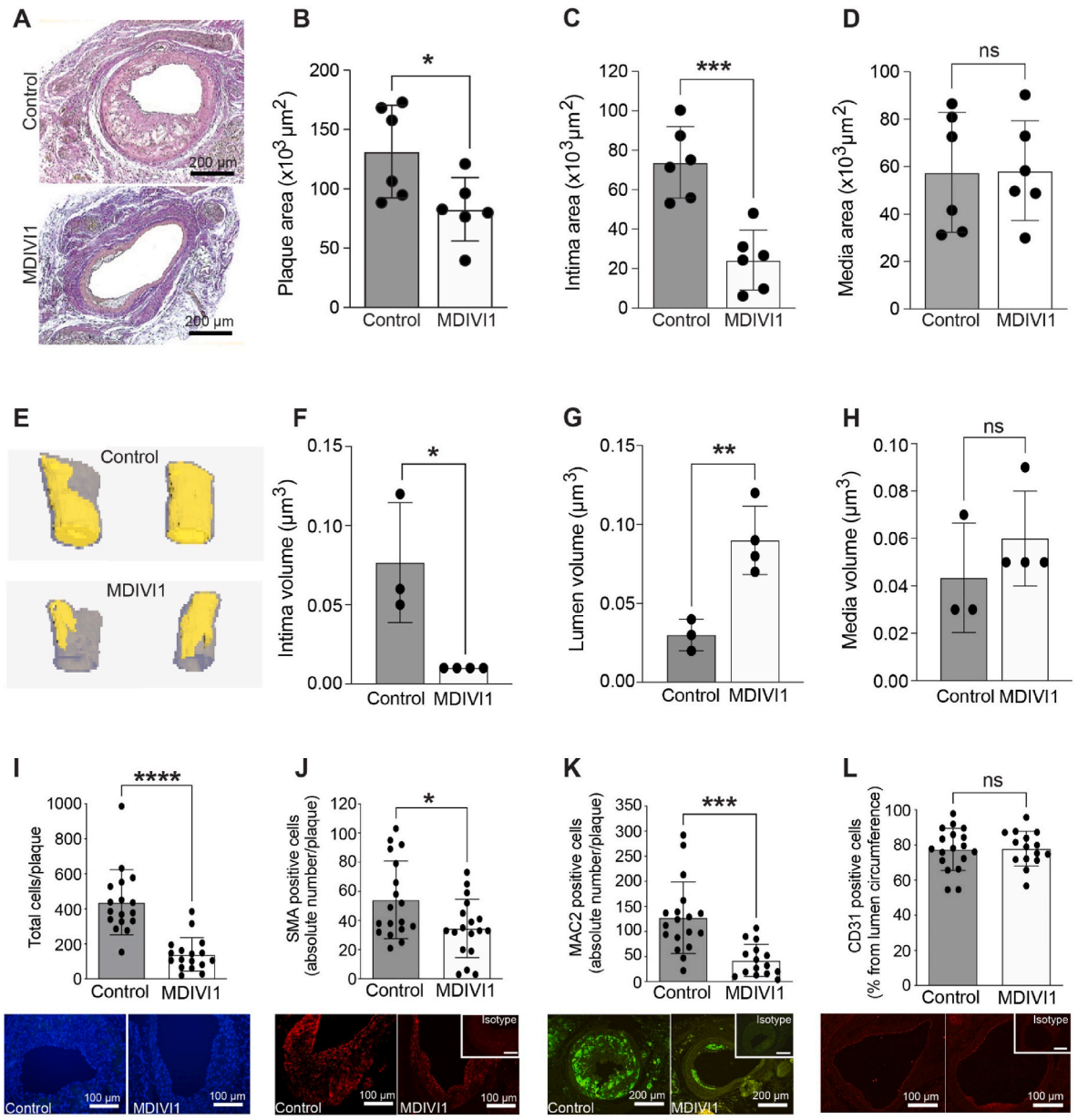

Fig. 1. Mdivi-1 treatment inhibited neointimal hyperplasia and reduced plaque complexity following wire-induced vascular injury.
(A) Representative photomicrographs of Pentachrome-stained sections 2 weeks after vascular injury in the presence or absence of Mdivi-1 treatment, scale bar 200 μm. Compared to control, treatment with Mdivi-1: reduced plaque area (B); decreased neointima area (C); but had no effect on medial area (D). (E) Representative 3D reconstructions of injured and uninjured arteries were analysed over 500 μm of vessel. Compared to control, treatment with Mdivi-1: reduced intima volume (F); increased lumen volume (G); had no effect on medial area (H); reduced the total number of plaque cells (DAPI), scale bar 100 μm (I); decreased the number of plaque smooth muscle cells (SMA$^+$), scale bar 100 μm (J); lowered the number of plaque macrophages (MAC2$^+$), scale bar 200 μm (K); but had no effect on the total number of plaque endothelial cells (CD31$^+$), scale bar 100 μm (L). Corresponding isotype control is represented in the inset. Values represent mean ± SD. *p* values (*p* values $^*p < 0.05$, $^{**}p < 0.01$, $^{***}p < 0.001$, $^{****}p < 0.0001$, ns – not significant) were assessed using Student *t* tests.

(same seeding density was used for BMDM). Cells were stimulated with the corresponding treatments for 6h and then the medium was changed to XF media (containing 5 mM HEPES), supplemented with 5.5 mM glucose, 2 mM glutamine and 1 mM sodium pyruvate and incubated for 1h at 37 °C with 0% CO_2 atmosphere prior to the experiment. The oxygen consumption rate (OCR) was recorded to assess mitochondrial respiratory activity. After three measurements under basal conditions, cells were treated sequentially with 1 μM oligomycin, 1 μM carbonyl cyanide p-(trifluoromethoxy) phenylhydrazone (FCCP) and 1 μM rotenone/antimycin A (seahorse biosciences), with three consecutive measurements under each condition that were subsequently averaged. Using Seahorse Wave software, metabolic parameters were obtained from the OCR profiling after subtraction of the rotenone/antimycin-insensitive respiration and normalized to the total amount of protein. Basal OCR is the oxygen consumption rate in the absence of effectors. ATP turnover was estimated from the difference between the basal and the oligomycin-inhibited respiration, and the maximal respiratory capacity was the rate in the presence of the uncoupler FCCP [29].

2.11. Cytokine arrays

Cytokines in cell culture supernatants from THP-1 monocytes and macrophages were determined using the human cytokine antibody array (Membrane, 23 targets; Abcam) with 23 different anti-cytokine/

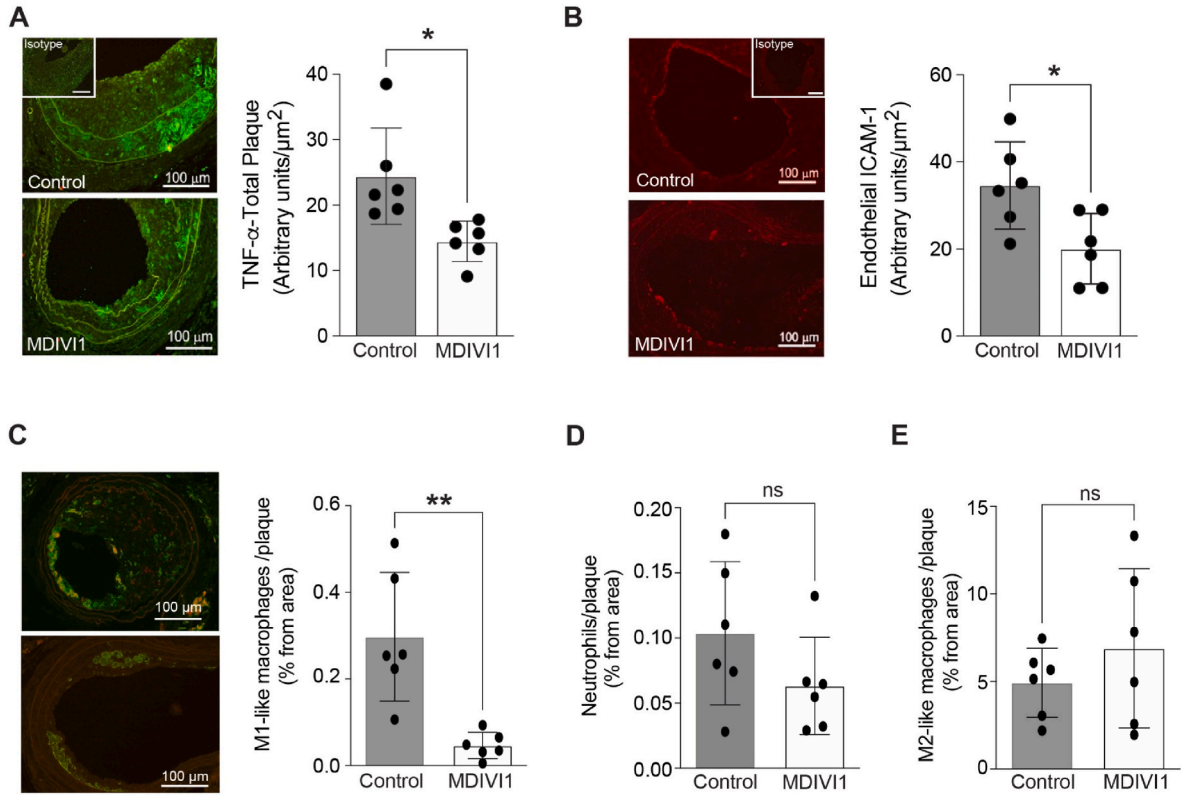

Fig. 2. Mdivi-1 treatment reduced vascular inflammation and endothelial activation after wire-induced vascular injury.
(A) Representative immunofluorescence images of TNF (Tumor necrosis factor)-α staining (green) in the plaque after vascular injury (scale bar 100 μm) showing Mdivi-1 treatment significantly reducing TNF-α levels when compared to control. (B) Representative immunofluorescence images of ICAM-1 (intercellular adhesion molecule 1) (red) at the luminal level after vascular injury (scale bar 100 μm) showing Mdivi-1 treatment significantly reducing plaque ICAM-1 levels. (C) Representative immunofluorescence of M1-like macrophages (Yellow), M2-like macrophages (Green) and neutrophils (Red) (scale bar 100 μm) 2 weeks after arterial injury showing Mdivi-1 treatment significantly reduced numbers of plaque M1-like ($MPO^+/MAC2^+$, yellow) macrophages, but with no effect on numbers of (D) plaque neutrophils (MPO^+, red) or (E) M2-like ($MAC2^+$, green) macrophages. Values represent mean ± SD. *p* values (*$p < 0.05$, **$p < 0.001$, ns – not significant) were assessed using Student *t* tests. (For interpretation of the references to colour in this figure legend, the reader is referred to the Web version of this article.)

chemokine antibodies spotted in duplicate on a nitrocellulose membrane according to manufacturer's protocol. Protein Array Analyzer tool from ImageJ was used for quantification, background correction and normalization of membrane signals as previous described [30]. The expression of cytokines/chemokines data was documented as their change in treated *versus* untreated (control) cells. The amount of TNFα and IL-6 in cell culture supernatants was determined using a human TNF-α ELISA (R&D Systems) and human IL-6 ELISA (Thermo Scientific) according to the manufacturer's protocols.

2.12. Metabolomic analysis

For metabolomics, THP-1 monocytes were incubated for 6h with Mdivi-1 or/and LPS + IFN-y to differentiate them towards M1-like phenotype. After incubation, the cells were washed with ice-cold PBS and suspended in 1:1 acetonitrile:water with 0.3% formic acid. Organic acids were extracted from the cell suspension, and their trimethylsilyl derivatives were quantitated by gas chromatography–mass spectrometry (GC-MS). Acylcarnitines and amino acids were extracted, and their methyl and butyl esters, respectively, were quantitated by liquid chromatography–mass spectrometry (LC-MS). Mass spectrometry analysis was performed by the Duke-NUS Metabolomics Core Facility. Results were normalized to total protein content.

2.13. Statistical analysis

GraphPad Prism for MAC (version 9) was used for all the statistical analyses. Differences were determined by one-way analysis of variance (ANOVA) with repeated measures, followed by *post-hoc* Bonferroni test where appropriate. Differences were considered significant when $p < 0.05$.

3. Results

3.1. Mdivi-1 treatment inhibited neointimal hyperplasia and reduced plaque complexity following wire-induced vascular injury

Treatment with Mdivi-1 reduced plaque area (Mdivi-1: 82.7 ± 10.9 × 10^3 μm^2 *vs.* control: 131.5 ± 15.9 × 10^3 μm^2, n = 6; p=0.03) and neointimal thickness (Mdivi-1: 24.4 ± 6.2 × 10^3 μm^2 *vs.* control: 73.9 ± 7.4 × 10^3 μm^2, n = 6; p=0.0004) in experimental mice compared with the control group (Fig. 1A–C), whereas tunica medial areas remained unchanged in both groups (Fig. 1D). Using our newly developed software to analyze 3D vascular segments, we confirmed that Mdivi-1 treatment reduced neointima thickness (Fig. 1E and F), increased the vascular lumen in the lesion (Fig. 1g) but did not affect tunica media thickness (Fig. 1H). There were fewer cells in plaques in the carotid artery after treatment with Mdivi-1 when compared to control (Mdivi-1: 147.1 ± 25.8 cells/plaque *vs.* control: 438.2 ± 45.0 cells/plaque, n = 6; p=0.0247; Fig. 1I). Additionally, vascular smooth muscle cells (SMA^+) (Mdivi-1: 35.6 ± 5.6 cells/plaque *vs.* control: 54.2 ± 6.3 cells/plaque, n = 6; p=0.0372; Fig. 1J) as well as macrophages ($MAC\text{-}2^+$) (Mdivi-1: 42.5 ± 8.3 cells/plaque *vs.* control: 127.5 ± 16.8 cells/plaque, n = 6; p=0.0042; Fig. 1K) were significantly decreased in the vascular lesions of Mdivi-1-treated mice compared to control. However, there were no significant differences in luminal endothelial cells ($CD31^+$) between

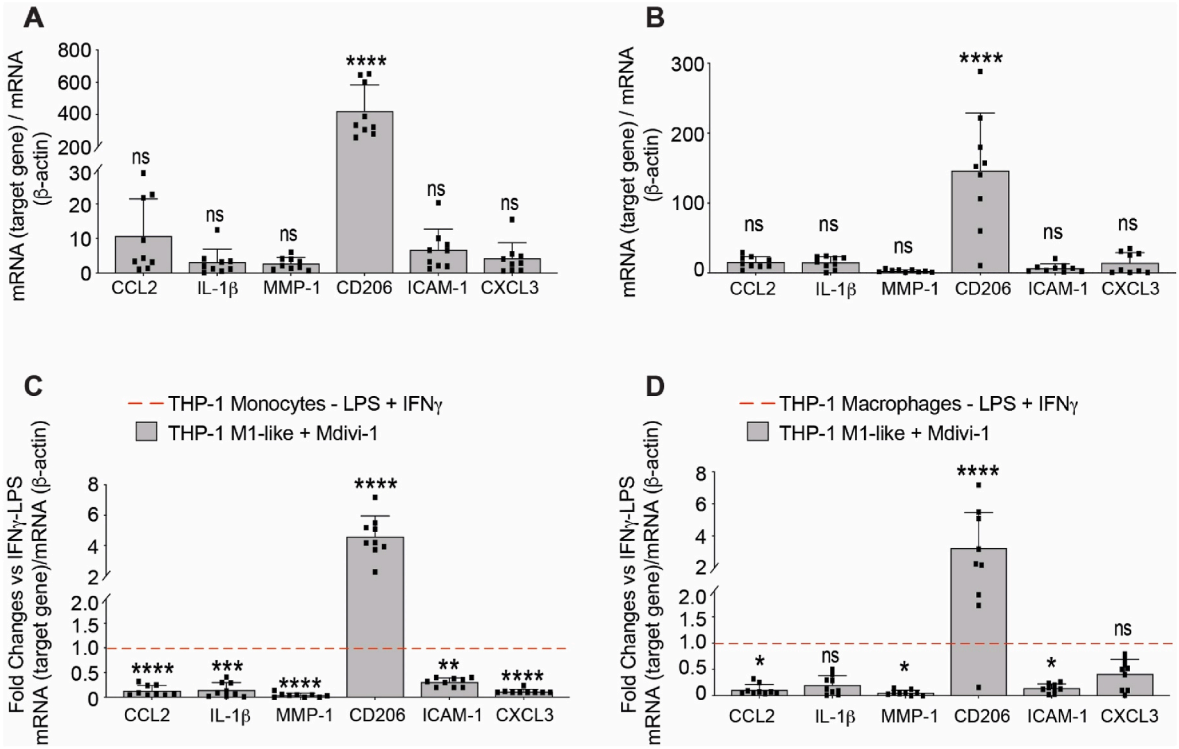

Fig. 3. Mdivi-1 treatment attenuated pro-inflammatory gene expression in THP-1 monocytes and macrophages.
Treatment of (A) THP-1 monocytes or (B) THP-1 macrophages with Mdivi-1 for 24 h increased mRNA expression of the anti-inflammatory cytokine, CD206, but did not affect levels of other cytokines, CCL2, IL-1β, MMP-1, ICAM-1 and CXCL3. (C and D) Gene expression data are normalized to LPS + IFN-γ treated group in the absence of Mdivi1 (dashed-red line) and displayed as fold changes between target gene expression and β-actin mRNA. Treatment of (C) THP-1 monocytes or (D) THP-1 macrophages stimulated with LPS + IFN-γ and Mdivi-1 significantly decreased mRNA levels of CCL2, IL-1β, MMP-1, ICAM-1 and CXCL3 and increased mRNA levels of CD206. Values represent mean ± SD (n = 3 per group in triplicates); *$p < 0.05$, **$p < 0.01$, ***$p < 0.001$, ****$p < 0.0001$, ns - not significant *vs.* DMSO (A, B) or LPS + IFN-γ treated cells (C, D) were assessed using 2way ANOVA and Bonferroni multiple comparisons post-test. (For interpretation of the references to colour in this figure legend, the reader is referred to the Web version of this article.)

treatment groups (Fig. 1L), demonstrating no differences in re-endothelialization between treatment groups. As expected, apoptosis was reduced in cells in the plaque, as assessed by TUNEL staining (Supplementary Fig. 1).

3.2. Mdivi-1 treatment reduced vascular inflammation and endothelial activation after wire-induced vascular injury

Mdivi-1 treatment reduced inflammation at the site of vascular injury compared to control, as evidenced by decreased plaque levels of the pro-inflammatory marker, TNF-α (Mdivi-1: 14.5 ± 1.6 arbitrary units/μm^2 *vs.* control: 24.4 ± 3.0 arbitrary units/μm^2, n = 6; p=0.0226; Fig. 2A). Similarly, Mdivi-1 reduced the levels of plaque-associated intercellular adhesion molecule-1 (ICAM-1), as a marker of endothelial activation (Mdivi-1: 20.4 ± 4.0 arbitrary units/μm^2 *vs.* control: 34.6 ± 4.1 arbitrary units/μm^2, n = 6; p=0.0367; Fig. 2B). Interestingly, Mdivi1 reduced the percent of pro-inflammatory macrophages in the plaque (Mdivi-1: 0.04 ± 0.01% *vs.* control: 0.29 ± 0.06%, n = 6; p=0.0023; Fig. 2C) without affecting the numbers of neutrophil and anti-inflammatory macrophage populations, suggesting a possible effect of Mdivi1 in macrophage polarization (Fig. 2D and E).

3.3. Mdivi-1 treatment attenuated pro-inflammatory gene expression in monocytes and macrophages

We next investigated the effect of Mdivi-1 on monocyte/macrophage polarization using the THP-1 monocyte cell line. Under basal conditions, THP-1 monocytes as well as THP-1 differentiated macrophages showed an upregulation of the mRNA expression of anti-inflammatory marker *CD206* (mannose receptor) after treatment with Mdivi-1, with initially no changes in pro-inflammatory target genes (Fig. 3A and B). During LPS + IFN-γ stimulation, Mdivi-1 prevented the polarization of THP-1 monocytes/macrophages towards M1-like phenotype, as demonstrated by the significant upregulation of *CD2*06 mRNA expression in both, THP-1 monocytes (Fig. 3C) and THP-1 differentiated macrophages (Fig. 3D). The switch from pro-inflammatory to an anti-inflammatory phenotype (M2-like polarization) was also evidenced by the decrease in the mRNA expression of pro-inflammatory chemokines and cytokines, such as CCL2, the chemokine (C-X-C motif) ligand 3 (CXCL3), *MMP*-1 (Matrix metalloproteinase-1), the adhesion molecule *ICAM-1* and *IL-1β* (Interleukin-1 β) in polarized THP-1 monocytes in the presence of Mdivi-1 (Fig. 3C). Similarly, the THP-1-derived macrophages demonstrated a significant decrease in mRNA levels of pro-inflammatory molecules, such as CCL2, *MMP-1,* and the adhesion molecule *ICAM-1* (Fig. 3D).

3.4. Mdivi-1 treatment reduced pro-inflammatory cytokines and chemokines in monocytes and macrophages

We next measured protein expression of cytokines in the supernatant of polarized THP-1 cells by ELISA in the presence or absence of Mdivi-1. The polarized THP-1 monocytes/macrophages towards M1-like phenotype under LPS + IFN-γ stimulation released high levels of TNF-α (Supplementary Fig. 2A) and IL-6 (Supplementary Fig. 2B) compared to their corresponding control (unstimulated cells), where the protein levels of both cytokines were below the detection level. Mdivi-1 treatment significantly reduced the protein levels of TNF-α and IL-6 in both monocytes (Fig. 4A) and macrophages (Fig. 4B) after short (6h) and long (24h) treatment period.

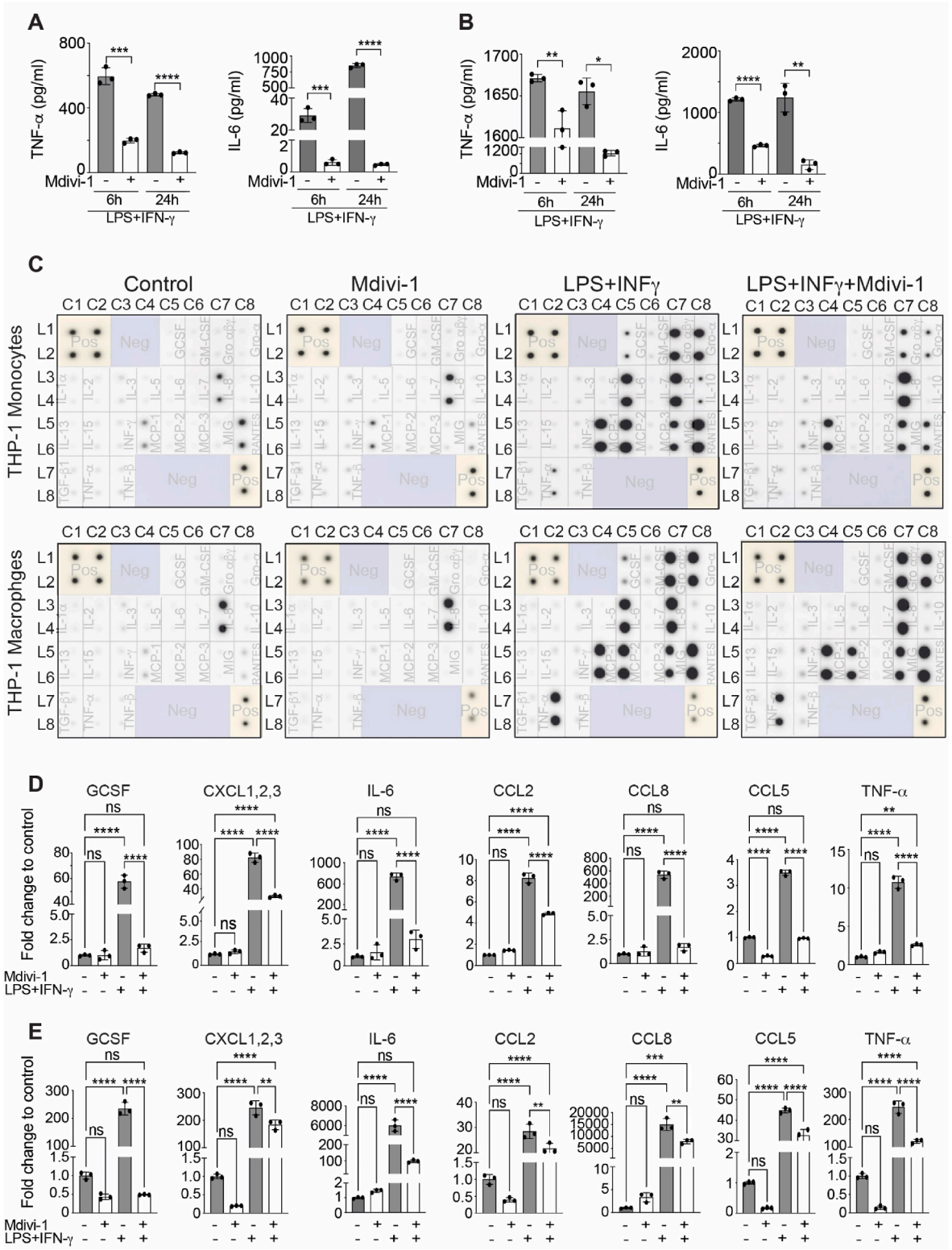

Fig. 4. Mdivi-1 treatment reduced pro-inflammatory cytokines and chemokines in THP-1 monocytes and macrophages.
Treatment of LPS + IFN-stimulated (A) THP-1 monocytes or (B) THP-1 macrophages with Mdivi-1 significantly decreased levels of TNF-α and IL-6 levels in the supernatant at 6 h and 24 h. (C) Representative membranes of a human cytokine antibody array analysing 23 cytokines from supernatant from untreated (control) and LPS + IFN-γ treated THP-1 monocytes (upper panel) and THP-1 macrophages (lower panel) with/without Mdivi-1. (D and E) The quantitative signal intensity of selected cytokines from THP-1 monocytes and macrophages, with changes in cytokine levels, are expressed as relative fold-change of the respective untreated control group. Mdivi-1 treatment of (D) THP-1 monocytes or (E) THP-1 macrophages attenuated the increase in GCSF, CXCL1,2,3, IL-6, CCL2, CCL8, CCL5, and TNF-α stimulated with LPS + IFN-γ, when compared to control. Values represent mean ± SD from three independent experiments. p values $^{**}p < 0.01$, $^{***}p < 0.001$, $^{****}p < 0.0001$, ns – not significant were assessed by 1-way ANOVA and Bonferroni multiple comparisons post-test. The readouts from densitometry scans were normalized using the intensity of positive control dots on the membrane corners and plotted as relative fold-change of the untreated control.

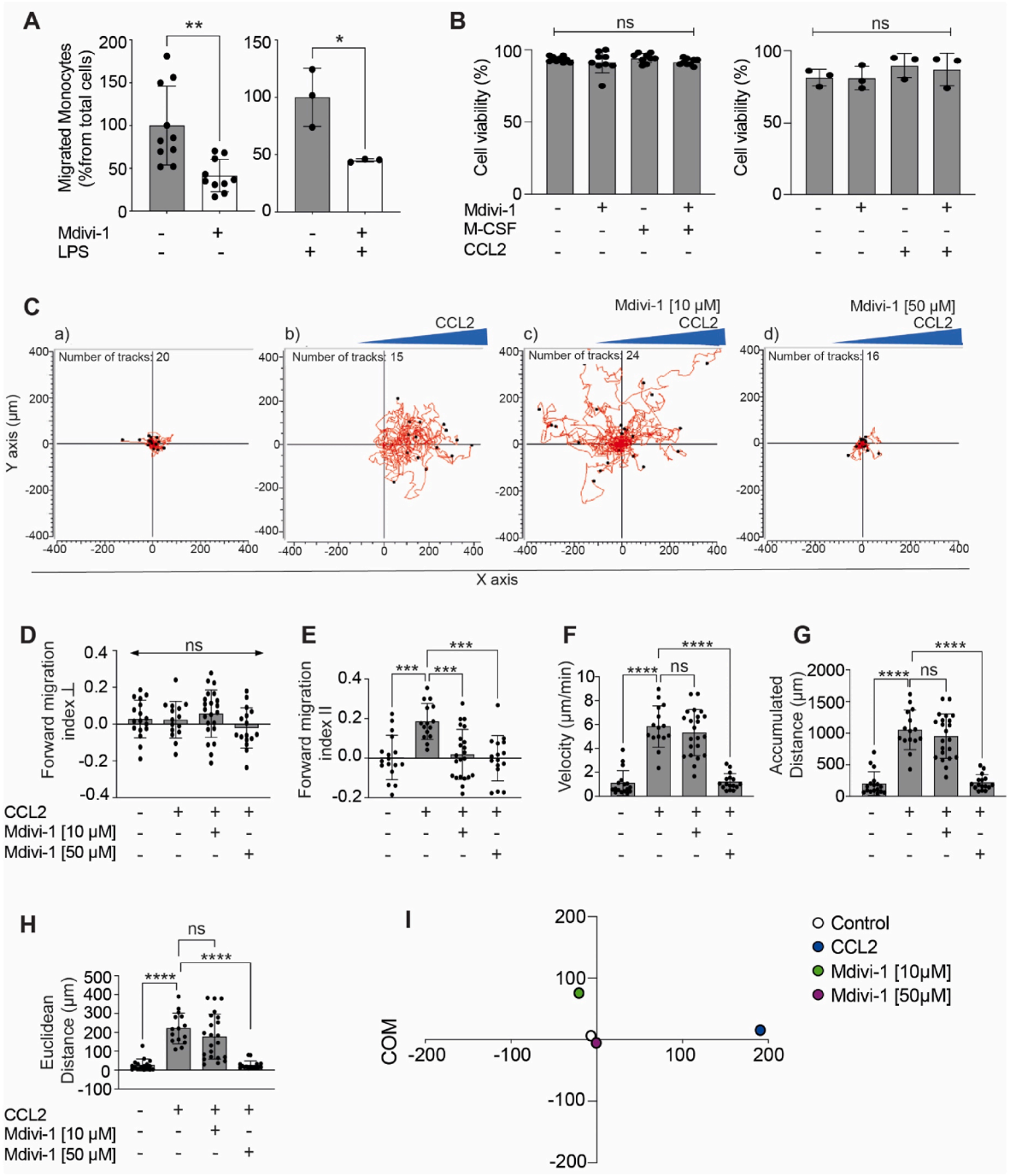

Fig. 5. Mdivi-1 treatment reduced migration and motility of THP-1 monocytes in response to chemoattractant.
(A) Mdivi-1 treatment significantly reduced the migration of resting (left panel) and LPS-activated (right panel) THP-1 monocytes in response to M-CSF in a transwell migration assays. Values represent mean ± SD. *p* values (*p* values $*p < 0.05$, $**p < 0.01$) were assessed using Student *t* tests. (B) Treatment of THP-1 monocytes (left panel) and human monocytes (right panel) with Mdivi-1 in the presence of M-CSF or CCL2 did not affect cell viability (values represent mean ± SD, 1-way ANOVA and Bonferroni's multiple comparison post-test was employed). (C) Representative figures showing multiple migration tracks of individual human monocytes in -a) control, -b) in the presence of MCP-1, -c) in the presence of CCL2 and Mdivi-1 (10 µM), and -d) in the presence of CCL2 and Mdivi-1 (50 µM). (D) As expected, the Forward migration index perpendicular to chemoattractant showed no effect of CCL2 or Mdivi-1 on monocyte migration. (E) Forward migration index parallel to chemoattractant showed significantly reduced chemotaxis-induced migration induced by CCL2 compared to control by the treatment of human monocytes with Mdivi-1 (50 µM). (F) CCL2 induced cell velocity was also significantly reduced by Mdivi-1 treatment. (G) Similarly, accumulated distance and (H) Euclidean distance calculated were reduced by Mdivi-1 treatment. (I) Representative image of centre of mass showing that Mdivi-1 treatment re-established the displacement induced by CCL2 stimulation. Values represent mean ± SD. *p* values $***p < 0.001$, $****p < 0.0001$, ns - not significant were assessed by 1way ANOVA and Bonferroni multiple comparisons post-test.

Table 1
Accumulated and Euclidean distance of human monocytes in a 3D chemotaxis assay.

Experimental groups	Accumulated distance (μm)	Euclidean distance (μm)
Control	202.6 ± 187.3	27.35 ± 31.19
MCP-1	1052 ± 313.2	221.0 ± 81.77
MCP-1 + Mdivi-1 [10 μM]	951.7 ± 350.9	177.6 ± 119.9
MCP-1 + Mdivi-1 [50 μM]	219.3 ± 122.9	26.11 ± 22.41

Besides TNF-α and IL-6, many other pro-inflammatory cytokines and chemokines were reduced after 24h Mdivi-1 treatment, as demonstrated by densitometry analysis of a semi-quantitative determination of 23 targets using a protein profiler (Fig. 4C–E, Supplementary Fig. 2C). Mdivi-1 treatment reduced significantly the pro-inflammatory mediators (G-CSF; CXCL1,2,3; IL-6; CCL2, CCL8; CCL5 and TNF-α) released by THP-1 monocytes (Fig. 4C and D) and THP-1 differentiated macrophages (Fig. 4C–E) in response to LPS + IFN-γ stimulation. Other proteins were minimally affected or not affected by the Mdivi-1 treatment (Supplementary Fig. 2D) in both, THP-1 monocytes (Supplementary Fig. 2E) and THP-1 differentiated macrophages (Supplementary Fig. 2F).

3.5. Mdivi-1 reduced the migration and motility of monocytes

We next investigated the effect of Mdivi-1 treatment on monocyte migration given that we had found reduced macrophage count in atherosclerotic plaques of mice treated with Mdivi-1 when compared to control. In a classic Boyden chamber (Transwell) assay, Mdivi-1 significantly reduced cell chemotaxis of resting and LPS-activated THP-1 monocytes in response to M-CSF (Fig. 5A). The reduced count number under Mdivi-1 treatment was not the result of increased cell death, since none of the experimental conditions affected the cell viability of the cells (Fig. 5B).

Further, using 3D chemotaxis assay, simulating a physiological environment (as illustrated in Supplementary Fig. 3A), cell motility was monitored by performing time-lapse imaging every 2 min using a Leica DMi8 M microscope (Leica, Germany) and analysed with manual tracking using the chemotaxis and migration tools from Ibidi GmbH (Munich, Germany) (Supplementary Fig. 3B). Primary human monocytes responded to the CCL2 gradient showing a homogenous directional migration (Fig. 5C–b), compared to the buffer control group (Fig. 5C–a). The treatment with a low concentration of Mdivi-1 (10 μM) reduced the directionality of the cell movement (Fig. 5C–c), whereas a high concentration (50 μM) of Mdivi-1 fully abrogated the migration behavior of monocytes towards the CCL2 gradient (Fig. 5C-d).

To exclude the possibility of random migration and to ensure that cell movement complied with the criteria for a directed/chemotactic cell migration, six different parameters were checked. First, the forward migration index (FMI), both perpendicular (Fig. 5D) and parallel (Fig. 5E) to the chemoattractant, was assessed with or without Mdivi-1. As expected, no differences were found in FMI perpendicular to CCL2, excluding the possibility of biased migration by non-chemotactic environmental factors. However, FMI parallel to chemoattractant was increased compared to control (Control: $3.5x10^{-3}$±0.1; CCL2: $1.85x10^{-1}$±0.09), and treatment with both concentrations of Mdivi-1 abolished the effect of CCL2 (Mdivi-1 [10 μM]: $1.89x10^{-2}$±0.126; Mdivi-1 [50 μM]: $3.21x10^{-4}$±0.11). Then, the influence of Mdivi-1 on chemotaxis velocity was studied, in which CCL2 induced a significant increase in cell velocity compared to the control (Fig. 5F), which was completely abrogated by treatment with 50 μM (Fig. 5F), but not by 10 μM Mdivi-1 treatment (Control: 1.11 ± 1.05 μm/min; CCL2: 5.84 ± 1.74 μm/min; Mdivi-1 [10 μM]: 5.33 ± 1.92 μm/min; Mdivi-1 [50 μM]: 1.22 ± 0.68 μm/min). Additionally, the expected increase in accumulated distance as well as the Euclidean distance induced by the chemoattractant were significantly attenuated by Mdivi-1 (50 μM) treatment, but not by Mdivi-1 (10 μM) (Table 1; Fig. 5G and H).

When assessing the Centre of Mass (COM), a displacement towards the CCL2-treated group compared to the control was noted (Fig. 5I), indicating that these cells primarily traveled in the direction of the chemoattractant. However, in the presence of Mdivi-1, this directional movement was abolished. These results are consistent with the Rayleigh test p values (Control: $p = 0.255$, CCL2: $p = 1.41x10^{-6}$, Mdivi-1 [10 μM]: $p = 0.191$ and Mdivi-1 [50 μM]: $p = 0.903$), indicating that the distribution of the cell endpoints was only significantly inhomogeneous (i.e., distributed towards the chemoattractant) in the presence of CCL2 alone. Collectively, these data indicate that Mdivi-1 modulates monocyte recruitment and chemotaxis and may limit the cellular transmigration capacity.

3.6. Mdivi-1 treatment inhibited mitochondrial respiration in THP-1 monocytes and macrophages

As metabolic remodeling plays a key role in cell polarization, the next step was to determine whether Mdivi-1 could modulate monocyte and macrophage oxidative metabolism and impact cell polarization status towards the M1-like or M2-like phenotypes. The determination of bioenergetics parameters was performed using the Seahorse system and the sequential use of mitochondrial complex modulators (Fig. 6A) such as oligomycin (mitochondrial ATP synthase inhibitor), FCCP (an uncoupling agent that collapses the proton gradient and disrupts the mitochondrial membrane potential) and a combination of rotenone and antimycin A (blockade of mitochondrial respiration by inhibiting complexes I and III, respectively), as previously described [29]. Both, M1-like (LPS + IFN-γ stimulated monocytes and macrophages) and M2-like (IL-4 stimulated macrophages) polarized cells exhibited a higher basal oxygen consumption rate (OCR) compared with unstimulated cells (DMSO), a difference that was abolished in the presence of Mdivi-1 (Fig. 6B–I). Moreover, maximal respiratory capacity in M1-like and M2-like monocytes/macrophages was increased compared to unstimulated cells, and the difference was abolished by the treatment with Mdivi-1 (Fig. 6C–J). Similar findings were observed in M1-like monocytes/macrophages and M2-like monocytes treated with Mdivi-1 when assessing ATP-linked respiration (Fig. 6 D, K). Further, Mdivi-1 treatment reduced the increase in reserve capacity (Fig. 6E–L) and non-mitochondrial respiration (Fig. 6F–M) in M1-like and M2-like monocytes and macrophages. Lastly, the increase in proton leak observed in both M1-like and M2-like monocytes was abolished in the presence of Mdivi-1 (Fig. 6G), while no differences were observed in proton leak in macrophages (Fig. 6N). The results were also reproduced in the primary isolated and differentiated bone marrow-derived macrophages (BMDM), where Mdivi-1 reduced the ATP-linked respirations and proton leak in M1-polarized cells (Supplementary Fig. 4).

3.7. Mdivi-1 treatment reprogrammed metabolism in THP-1 monocytes

To further explore the changes seen in oxygen consumption in the presence of Mdivi-1, a metabolomic analysis was performed to investigate the influence of Mdivi-1 treatment on main metabolic pathways involved in monocyte polarization, such as TCA cycle organic acids, amino acids, and acylcarnitine metabolism. Characteristic for the M1-like differentiated monocytes, succinate levels increased significantly, while amino acids, such as arginine and citrulline were depleted in our model, as detected by LC-MS. Remarkably, Mdivi-1 effectively prevented the succinate accumulation while restoring the levels of arginine and citrulline in M1-like monocytes (as shown in Fig. 7A). This is vital for preserving mitochondrial homeostasis, sustaining cellular energy levels, and ensuring proper cellular function. While not affected by the LPS + IFN-γ polarization stimulus, we found that Mdivi-1 treatment reduced the main components of the TCA-cycle in THP-1 monocytes, such as α-ketoglutarate, succinate, fumarate, malate, and citrate (Fig. 7B), impairing their accumulation and probably reducing the pro-

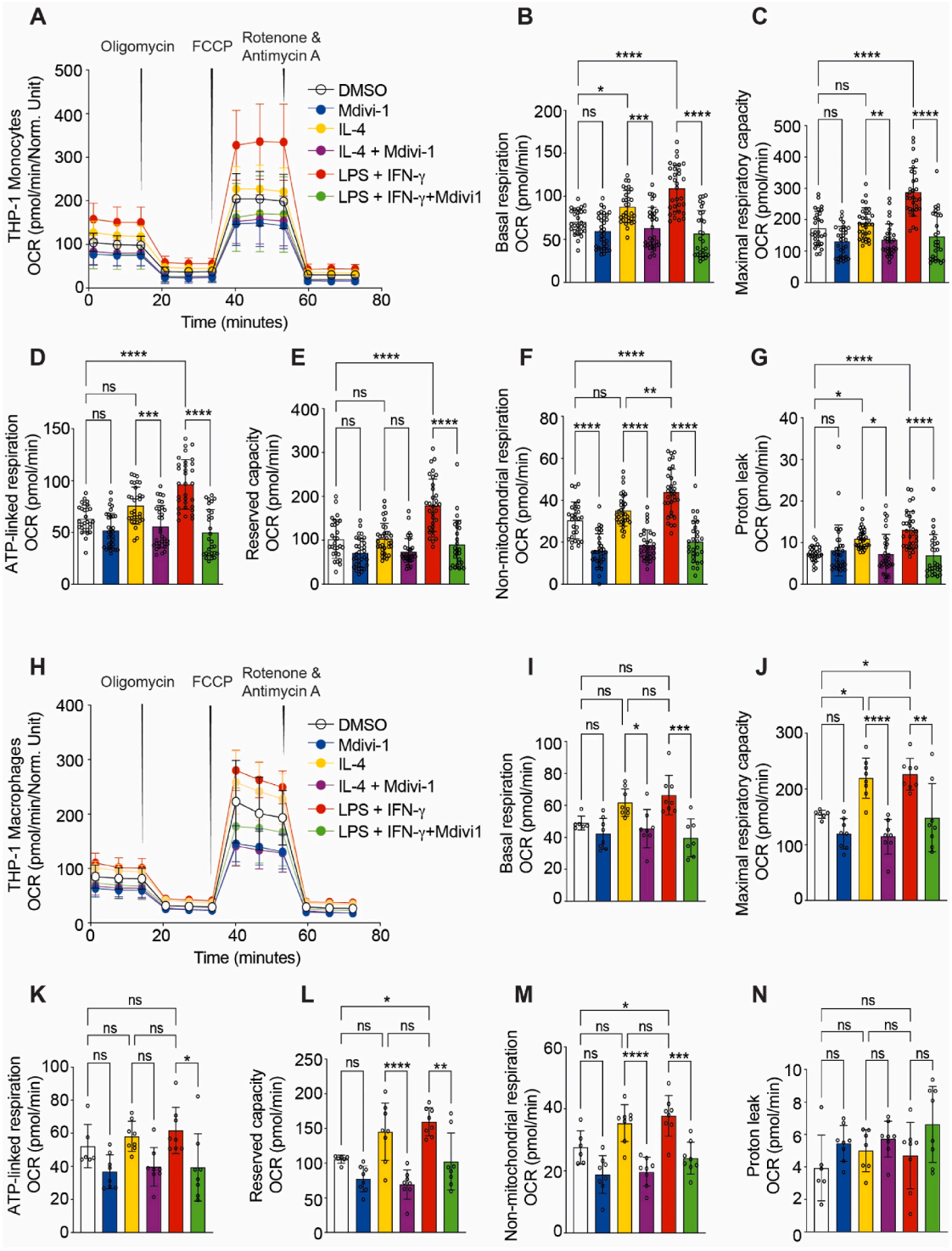

Fig. 6. Mdivi-1 treatment inhibited mitochondrial respiration in THP-1 monocytes and macrophages.
(A) Representative time-dependent courses of oxygen consumption rate (OCR) measured with the Seahorse XFe96 metabolic analyser in THP-1 monocytes polarized to M1-like (LPS + IFN-γ) or M2-like (IL-4) phenotype and untreated (control) cells for 6h, in the presence or absence of Mdivi-1 were subjected to serial injections of oligomycin (ATP production), FCCP (Maximal respiration) and antimycin A/rotenone. Effects on (B) basal respiration, (C) maximal respiratory capacity, (D) ATP-linked respiration, (E) reserve capacity, (F) non-mitochondrial respiration and (G) proton leak are depicted separately. (H) Representative time-dependent courses of OCR measured with the Seahorse XFe96 metabolic analyser in THP-1 macrophages polarized to M1-like (LPS + IFN-γ) or M2-like (IL-4) phenotype and untreated (control) cells for 6h, in the presence or absence of Mdivi-1 were subjected to serial injections of oligomycin (ATP production), FCCP (Maximal respiration) and antimycin A/rotenone. Effects on (I) basal respiration, (J) maximal respiratory capacity, (K) ATP-linked respiration, (L) reserve capacity, (M) non-mitochondrial respiration, and (N) proton leak are depicted separately. Overall, treatment of THP-1 monocytes and macrophages with LPS + IFN-γ increased mitochondrial respiration, and this effect was attenuated by treatment with Mdivi-1. Treatment with Mdivi-1 also decreased mitochondrial respiration in THP1 monocytes and macrophages stimulated with IL-4. Values represent mean ± SD (THP-1 monocytes n = 28–32 wells analysed per group; THP-1 macrophages n = 6–8 wells analysed per group); *$p < 0.05$; **$p < 0.01$; ***$p < 0.001$; ****$p < 0.0001$, ns - not significant were assessed by 1way ANOVA and Bonferroni multiple comparisons post-test.

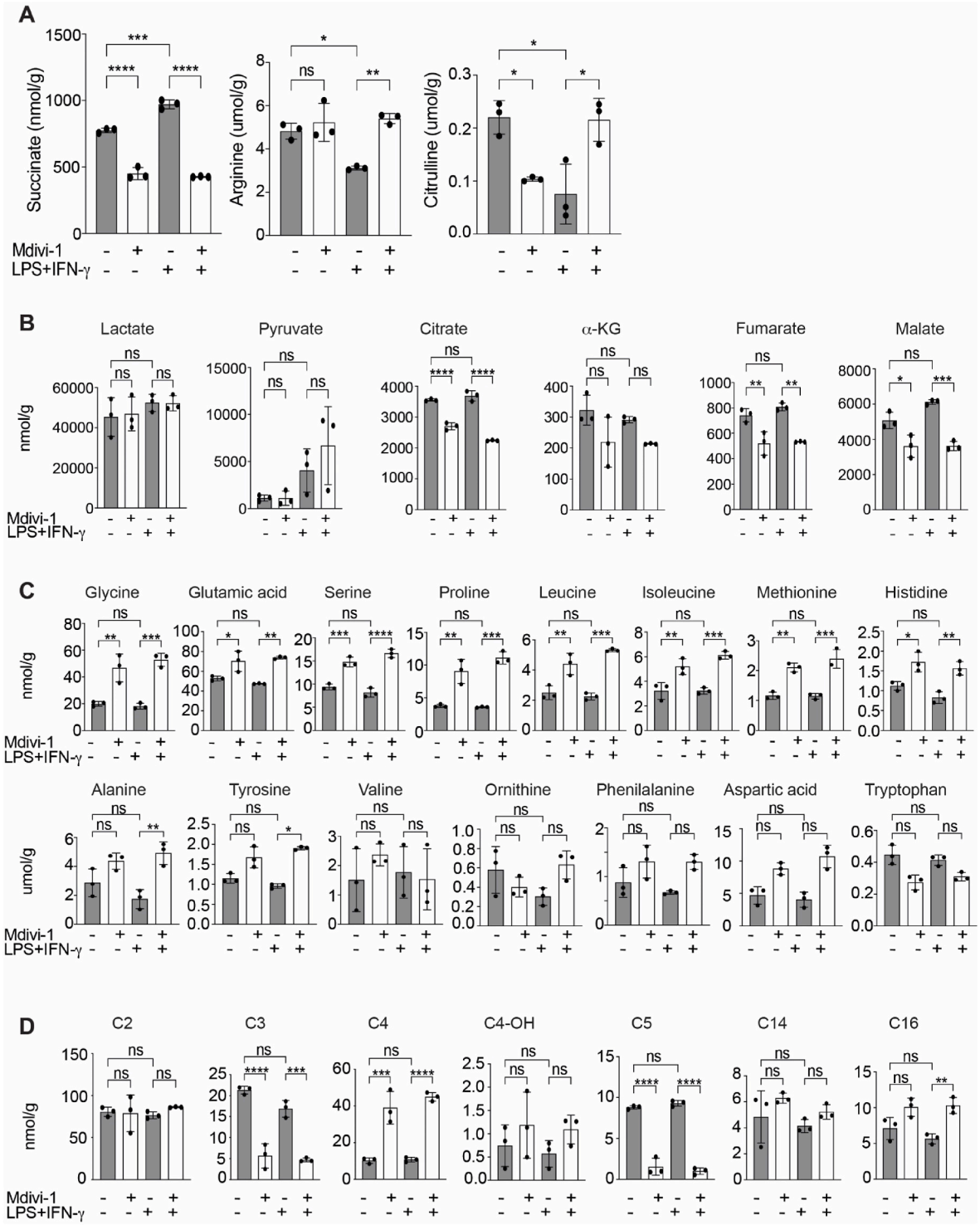

Fig. 7. Metabolomic changes in THP-1 monocytes with/without Mdivi-1 treatment.
(A) Treatment of THP-1 monocytes with LPS + IFNg to induce M1-like polarization increased levels of succinate and reduced levels of arginine and citrulline. Treatment with Mdivi-1 alone significantly reduced succinate and citrulline levels but had no effect on arginine levels. Treatment with Mdivi-1 of THP-1 monocytes stimulated by LPS + IFNg significantly reduced succinate and significantly increased both arginine and citrulline levels. (B) Mdivi-1 treatment reduces the main components of the TCA-cycle in THP-1 monocytes, such as α-KG, succinate, fumarate, malate, and citrate. (C) Mdivi-1 increased the availability of different amino acids. (D) Mdivi-1 influenced particularly the short-chain acylcarnitine fraction in acylcarnitine metabolism. Values represent mean ± SD (n = 3); *$p < 0.05$; **$p < 0.01$; ***$p < 0.001$; ****$p < 0.0001$, ns - not significant were assessed by 1way ANOVA and Bonferroni multiple comparisons post-test.

inflammatory phenotype [31]. Also not related to the M1-like polarization, Mdivi-1 was able to increase the availability of the amino acids, which are essential for cellular function and homeostasis (Fig. 7C) [32]. Further, Mdivi-1 influenced particularly the short-chain acylcarnitine fraction in acylcarnitine metabolism, responsible for activating the alternative energy sources (Fig. 7D), unrelated to polarization processes.

3.8. Mdivi-1 treatment had no effect on mitochondrial morphology in monocytes

Given the role of Mdivi-1 as a putative Drp1 inhibitor, we investigated the effect of Mdivi-1 on mitochondrial morphology in THP-1 monocytes undergoing M1/M2-like polarization. There was a non-significant increase in mitochondrial fusion with Mdivi-1 treatment compared to the control, but no differences were found in mitochondrial morphology in any of the other groups (Supplementary Figs. 5A and B). These results correlated with the phosphorylation status of Drp-1 (Ser616/Ser637) as assessed by Western blot analysis (Supplementary Figs. 5C and D) in which no significant changes were seen in LPS + IFN-γ-treated monocytes in the presence or absence of Mdivi-1. These data indicate that the observed effects of Mdivi-1 on bioenergetics in human monocytes appear to be independent of changes in mitochondrial morphology and Drp-1 phosphorylation.

4. Discussion

The present study shows for the first time that treatment with Mdivi-1 significantly reduced neointimal hyperplasia, decreased monocyte recruitment into the plaque, and reduced vascular inflammation after carotid wire injury in *Apoe*$^{-/-}$ mice, fed a high-fat diet. These findings were accompanied by metabolic changes in monocytes and macrophages including decreased oxidative metabolism. The carotid wire-induced endothelial denudation mouse model is a widely used experimental procedure to induce tunica intimal hyperplasia and recapitulates the restenosis process seen in CAD and PAD patients undergoing angioplasty and stent procedures [18]. HFD-fed *Apoe*$^{-/-}$ mice subjected to endothelial denudation showed marked neointimal hyperplasia after two weeks of injury [17,18] that was accompanied by an increase in cellularity in the vascular lesion. In this model, Mdivi-1 treatment reduced neointimal hyperplasia and significantly decreased vessel wall thickness; findings that were associated with reduced plaque complexity due to decreased cell infiltration. Mdivi-1 treatment also lowered the number of macrophages and VSMCs recruited into the plaque area.

In this regard, our *in vivo* data correlate well with a recent study showing that genetic deletion of Drp1 in macrophages in mice significantly reduced intimal thickening and macrophage infiltration during femoral injury-induced vascular remodeling [33], although mice used in this study contained functional Apoe and were not administered an atherogenic diet as in our experimental mice. Furthermore, the *Cre* recombinase system used to induce the genetic ablation of Drp1 in macrophages also targeted the neutrophil population, and it is therefore expected that the inflammatory response after vascular injury in these mice was less severe when compared to our *in* vivo model of carotid-wire injury. All these findings reveal a favorable effect of Mdivi-1 administration on vascular remodeling following wire-induced endothelial injury that was accompanied by a significant reduction of VSMCs and macrophage infiltration in the plaque.

It has been reported that, following endothelial denudation, increased levels of the chemoattractant protein CCL2 and M-CSF are released at the site of vascular injury, mediating the recruitment of monocytes from the circulation and their later differentiation into macrophages [34–37] which is known to be a strong determinant for the progression of neointimal formation [36,38]. Our *in vitro* data showed that Mdivi-1 reduced monocyte chemotaxis and transmigration in response to both, CCL2 and M-CSF. In line with these findings, recent data have shown that Mdivi-1 could downregulate the expression of the CCL2 receptor (CCR2) in murine macrophages [33]. Also, our semi-quantitative protein determination showed a decreased production of CCL2 and CCL8 in LPS/IFN-γ-treated monocytes and macrophages, indicating that Mdivi-1 may be preventing cell migration via modulation of the CCL2/CCR2 pathway. This data correlates very well with the reduction in macrophage content found in the plaques of mice treated with Mdivi-1 when compared to control.

Macrophages have been classically identified as the source of TNF-α after vascular injury [39]. Consistent with this observation, the analysis revealed an anti-inflammatory response following Mdivi-1 treatment *in vivo*, with lowered levels of TNF-α and reduced expression of the adhesion molecule ICAM-1 in the vascular lesion. Adhesion molecules such as ICAM-1, V-CAM-1, and P-selectin are highly expressed after mechanical denudation of the vessel and are involved in the severity of the neointimal hyperplasia [40–42] due to their roles in mediating inflammatory cell recruitment to the site of injury [43–45]. Consistent with this data, our control mice (DMSO-treated) expressed the atherogenic adhesion molecule ICAM-1 in the vasculature after denudation. It has been reported that ICAM-1 is transcriptionally regulated by TNF-α in the endothelium in a NFκB-dependent manner [46–48] and that TNF-α production is post-transcriptionally regulated by Drp-1 in macrophages [49]. Hence, we hypothesize that Mdivi-1 may be modulating this regulatory mechanism which could explain the decreased levels of TNF-α and ICAM-1 seen in the carotid arteries after endothelial denudation. Together, these findings underline the properties of Mdivi-1 as an anti-inflammatory drug under conditions of vascular injury *in vivo*.

Inflammation-related factors released by monocytes and macrophages, including cytokines and chemokines, are implicated in the initiation and progression of neointimal hyperplasia after vascular injury [50,51]. Here, *in vitro* evidence is provided in human THP-1 monocytes and THP-1-derived macrophages, showing that Mdivi-1 reduced the expression and production of several cytokines and chemokines following polarization to a M1-like phenotype using LPS/IFN-γ. Hence Mdivi-1 is promoting an M2-like phenotype that was evidenced by the upregulation of the M2-like marker CD206. As expected, levels of both TNF-α and IL-6 were higher in the macrophage population when compared to monocytes after stimulation with LPS + IFN-γ. This effect has been associated with a more susceptible response to pro-inflammatory stimuli of THP-1 cells after PMA treatment which induced the macrophage-like phenotype in these cells [52–54].

In agreement with our findings, the anti-inflammatory effect of Mdivi-1 has been reported *in vitro* in different cell types, such as epithelial cells, T cells, endothelial cells, microglia, and murine macrophages [55–58] as well as *in vivo* in a recent study using a murine model of diet-induced atherosclerosis [59]. Despite the overall anti-inflammatory function mediated by Mdivi-1 in these cells, THP-1 cells showed a constitutive production of CXCL8, which has been previously reported in leukemic myelocytic cells as well [60,61], and Mdivi-1 seemed to enhance this basal production. However, in THP-1 cells under inflammatory conditions (LPS/IFN-γ) this behaviour was not seen in the presence of Mdivi-1. Since this cytokine (IL-8) has been identified as an autocrine/paracrine growth factor for human hematopoietic progenitors, leading to growth and differentiation of cells of monocytic lineage [62], we propose that Mdivi-1 treatment potentiates these effects on THP-1 cells under basal conditions, but not after pro-inflammatory stimulation.

Given that changes in mitochondrial function are known to contribute to alterations in the immune response [63], we evaluated whether changes in mitochondrial function and metabolism could be associated with the observed anti-inflammatory effects of Mdivi-1. Recent studies have reported that metabolic changes in macrophages may be used to assess the polarization status of these cells. Typically, M1-like macrophages display enhanced glycolytic metabolism and reduced mitochondrial activity, while anti-inflammatory M2-like macrophages show high mitochondrial oxidative phosphorylation and are characterized by an enhanced spare respiratory capacity (SRC) [64–66]. In contrast, our results reveal that oxidative metabolism was highly stimulated in M1-like monocytes and macrophages, while Mdivi-1 could suppress this response, the findings of which may be explained as follows:

The metabolic reprogramming of mitochondria after an inflammatory stimulus has been studied in cells from myeloid linage, classifying them as early (0–6h), sustained (up to 24h), or tolerant (24h stimulation

followed by another 10–24h) response [67]. Our data indeed displayed the phenotype of an early response. In line with this, monocytes and macrophages isolated from patients with atherosclerotic CAD showed higher mitochondria activity after stimulation (3h) with LPS/IFN-γ, presenting significantly higher OCR when compared to control. Also, the glycolytic flux in the same cells was markedly elevated as reflected by increased ECAR values [68]. Another study showed enhanced basal OCR and SRC in human monocytes after LPS treatment (4h) [69]. The mechanism behind this finding was recently described by Langston et al. [70], who showed an increased oxidative metabolism and high glucose oxidation during acute LPS exposure of bone marrow-derived macrophages. This response was due to the enhanced activity of the mitochondrial glycerol 3-phosphate dehydrogenase (GPD2), a component of the glycerol phosphate shuttle (GPD), which drives forward electron transport (FET) in the electron transport chain and fueled the production of acetyl coenzyme A, enhancing acetylation of histones and inflammatory gene induction in these cells.

This raises the possibility that the reduced oxidative metabolism seen in the presence of Mdivi-1 in both monocytes and macrophages may be due to the modulation of this adaptive mechanism of the mitochondria. However, in contrast to our results, Umezu et al. reported in murine macrophages neither an increase nor a decrease in mitochondrial respiration after exposure to LPS/IFN-γ alone or with and without Mdivi-1 [33]. Other studies in cancer cells have reported both a reduction [71,72] and an elevation [73] of oxidative metabolism after Mdivi-1 treatment. Additionally, human smooth muscle cells [74] and mouse neuroblasts [75] have shown increased OCR in the presence of Mdivi-1. The discordant findings may be due to the difference in cell type, culture conditions, Mdivi-1 concentration and treatment duration, or the metabolic assay used to assess mitochondrial respiration.

Alterations in mitochondrial functions have been associated with changes in mitochondrial morphology, and it is well accepted that enhanced fission activity leads to mitochondrial fragmentation and impaired OXPHOS, whereas increased fusion activity leads to an enhanced oxidative metabolism [76]. As such, we investigated whether the observed metabolic effects of Mdivi-1 were associated with changes in mitochondrial morphology in THP-1 monocytes. Unexpectedly, treatment with Mdivi-1 only induced changes in mitochondrial morphology in basal unstimulated cell and had no significant effect in either mitochondrial morphology or Drp1 phosphorylation (at Ser616 and Ser637), suggesting that the observed metabolic effects of Mdivi-1 were independent of changes in mitochondrial morphology or Drp1 phosphorylation status.

High levels of mitochondria fragmentation were displayed in THP-1 cells under basal conditions, which may be due to a constitutive IL-8 production found in THP-1 cells, since this interleukin has been reported to increase mitochondrial fragmentation in *in vitro* cultured cells [77]. In contrast, other studies have reported an increase in mitochondrial fragmentation with enhanced phosphorylation of Drp1-Ser616 in murine macrophages after LPS stimulation, and such changes were reversed by treatment with Mdivi-1 alone [33] or in combination with another fusion promoter molecule [78]. On the other hand, morphometric analysis of mitochondria in primary human monocytes and THP-1-macrophages subjected to pro-inflammatory stimulation (LPS/IFN-γ) displayed elongated fused mitochondria [69,79]. The latter findings are consistent with our data in which LPS/IFN-γ treated THP-1 monocytes had a trend to increase mitochondrial fusion, even though the data was not statistically significant.

Finally, succinate and arginine metabolism also play important roles in the polarization of monocytes and macrophages, thereby influencing the immune response. While M1-like macrophages use arginine to produce nitric oxide and citrulline upon pro-inflammatory exposure [80], M2-like macrophages preferentially metabolize arginine into ornithine, which supports tissue repair and collagen synthesis [81]. Further, succinate is a key feature of M1-like polarization and is associated with the production of pro-inflammatory cytokines, increased glycolysis, and reduced mitochondrial respiration [82]. The accumulation of succinate in M1-like macrophages stabilizes HIF-1α, promoting the release of pro-inflammatory cytokines [83,84]. Additionally, succinate is known to induce reverse electron transport (RET) at mitochondrial respiratory complex I and drive pro-inflammatory ROS signal in LPS-activated macrophages. Notably, inhibition of complex I with substances like rotenone significantly reduces LPS-induced ROS levels [85].

M2-macrophages shift away from glycolysis and succinate accumulation, thus increasing their anti-inflammatory capacity and promoting tissue-regeneration [86,87]. We found a significant accumulation of succinate as well as reduced levels of arginine in M1-like macrophages, as previously reported [88]. Similarly, citrulline levels were reduced, which should be important for an adequate immune response [89]. Notably, Mdivi-1 was able to effectively restore the arginine and citrulline levels to those seen in the control group and to reduce accordingly the succinate level. Moreover, even if there were no significant differences in TCA cycle metabolites between the control and M1-macrophages in our model, Mdivi-1 still reduced significantly the level of fumarate, malate, and citrate, which demonstrated the impact of Mdivi-1 on the polarization process. This data provides additional support for the role of Mdivi-1 in regulating and stabilizing the polarization of macrophages towards an M2-like phenotype, thus representing a valuable therapeutic strategy to impair neointima formation after vascular injury.

Taking together, this data indicates that the anti-inflammatory effect linked to reduced mitochondria respiration seen in THP-1 cells after Mdivi-1 treatment may be related to its inhibitory action on mitochondria complex I and the reduced production of reactive oxygen species, instead of its putative role as a Drp1 inhibitor, adding evidence to some of its proposed off-targets effects [13,90]. This hypothesis is supported by experimental evidence showing the role of ROS during neointimal hyperplasia after vascular injury, promoting cell proliferation, migration, and apoptosis [91–95]. In line with this, our control mice showed increased levels of TdT-mediated dUTP nick end labelling (TUNEL), an indicator of apoptosis, and such elevation was reduced by Mdivi-1 treatment. Therefore, we can assume that the reduced mitochondrial respiration after Mdivi-1 administration may lower the production of ROS via inhibition of mitochondria complex I, protecting it from ROS-mediated apoptosis. This hypothesis is also supported by a recent study showing that pharmacological inhibition of mitochondria complex I could attenuate neointimal hyperplasia after vascular injury via modulation of cell proliferation and migration, possibly by reducing ROS production [96]. However, further studies are needed to elucidate the mechanisms by which Mdivi-1 potentially modulates ROS-induced neointimal hyperplasia.

There are several limitations of our study as follows: First, the wire-induced injury was performed in healthy blood vessels that lack established atherogenic pathology, which differs from the clinical setting in which angioplasty or stenting is performed in a diseased vasculature. Second, while most of our experiments were performed on THP-1 cells, there are well-known differences between these immortalized cells and the primary human monocytes [97], and therefore, more validation is needed using blood-derived monocytes to draw more definitive conclusions. Third, we focused on the monocyte/macrophage population, while more studies are needed to elucidate the protective effect of Mdivi-1 on VSMCs during vascular injury. Lastly, our results suggest that Mdivi-1 acts by a mitochondrial dynamics-independent mechanism, but whether it acts through Drp-1 or not remains an open question. Therefore, due to the off-target effects of Mdivi-1, further studies are needed using agents that are more Drp1-specific such as Drpitor1 or Drpitor1a [98] to better understand the role of this mitochondrial fission protein during vascular restenosis. Nevertheless, despite these limitations, our results provide new insights into the interplay between mitochondrial function and modulation of the inflammatory response during vascular injury. Additional studies are required in this field for a complete and greater comprehension of the function of mitochondria and their

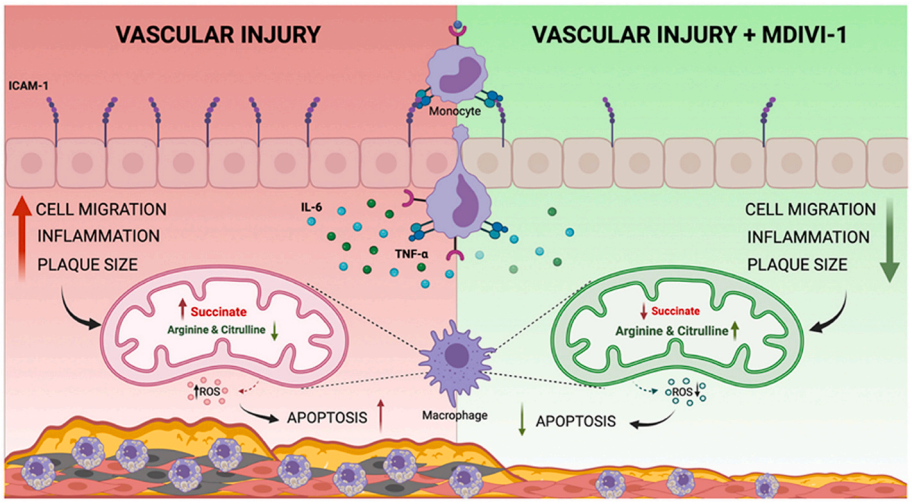

Fig. 8. Mechanical vascular injury induces an increase in neointima hyperplasia with cell migration, secretion of inflammatory cytokines, expression of adhesion molecules, induction of pro-inflammatory macrophages with enhanced oxidative phosphorylation, and perturbation of metabolites (succinate, arginine, and citrulline). Mdivi-1 treatment inhibited post-vascular injury neointimal hyperplasia, reduced plaque size, suppressed inflammation, inhibited oxidative phosphorylation and shifted pro-to anti-inflammatory macrophages, and corrected metabolite levels (succinate, arginine, and citrulline).

influence on inflammation during vascular restenosis.

In conclusion, we describe here for the first time that Mdivi-1 strongly protects against neointimal hyperplasia following endothelial wire-injury where it has beneficial effects on vascular remodeling by metabolic reprogramming of monocytes/macrophages from a pro-inflammatory to anti-inflammatory phenotype, potentially through Drp1-independent mechanisms (see Fig. 8). As such, metabolic modulation of monocyte and macrophage polarization using Mdivi-1 may thereby provide a new therapeutic strategy for inhibiting post-angioplasty restenosis in patients with CAD and PAD.

Financial support

Chrishan Ramachandra was supported by the SingHealth Duke-NUS Academic Medicine Research Grant (AM/TP033/2020 [SRDUKAMR2033]) and the Khoo Bridge Funding Award (Duke-NUS-KBrFA/2022/0059). Shengjie Lu is supported by the Singapore Ministry of Health's National Medical Research Council under Open Fund–Young Individual Research Grant (OF-YIRG, MOH-000230). Elisa Liehn was supported by the Ministry of Research, Innovation and Digitization, CNCS - UEFISCDI, project number PN–III–P4-PCE-2021-1680, within PNCDI III. Jürgen Bernhagen was supported by the Deutsche Forschungsgemeinschaft (DFG), grant SFB1123-A3, and the LMUexc strategic partnerships with Singapore. Derek Hausenloy is supported by the Duke-NUS Signature Research Programme funded by the Ministry of Health, Singapore Ministry of Health's National Medical Research Council under its Singapore Translational Research Investigator Award (MOH-STaR21jun-0003), Centre Grant scheme (NMRC CG21APR1006), and Collaborative Centre Grant scheme (NMRC/CG21APRC006). This article is based upon work supported by the National Research Foundation Competitive Research Program (NRF CRP25-2020RS-0001) and COST Actions EU-CARDIOPROTECTION IG16225 and EU-METAHEART CA22169 supported by COST (European Cooperation in Science and Technology). This work is part of the doctoral thesis of Gustavo E. Crespo-Avilan at the Justus-Liebig-University, Giessen, Germany.

CRediT authorship contribution statement

Gustavo E. Crespo-Avilan: Design of the study, performed the experiments, analysis and result interpretation, wrote the manuscript. **Sauri Hernandez-Resendiz:** performed the experiments, analysis and result interpretation, wrote the manuscript. **Chrishan J. Ramachandra:** performed the experiments, analysis and result interpretation, wrote the manuscript. **Victor Ungureanu:** Performed the 3D reconstruction of the carotid arteries, performed automatic analysis and result interpretation. **Ying-Hsi Lin:** analysis and result interpretation, wrote the manuscript. **Shengjie Lu:** analysis and result interpretation, wrote the manuscript. **Jürgen Bernhagen:** performed the experiments. **Omar El Bounkari:** performed the experiments. **Klaus T. Preissner:** Design of the study, analysis and result interpretation, wrote the manuscript. **Elisa A. Liehn:** Design of the study, performed the experiments, analysis and result interpretation, wrote the manuscript. **Derek J. Hausenloy:** Design of the study, analysis and result interpretation, wrote the manuscript.

Declaration of competing interest

The authors declare that they have no known competing financial interests or personal relationships that could have appeared to influence the work reported in this paper.

Acknowledgments

The authors wish to thank Dr. Hector A. Cabrera-Fuentes for his scientific input.

Appendix A. Supplementary data

Supplementary data to this article can be found online at https://doi.org/10.1016/j.atherosclerosis.2024.117450.

References

[1] S. Barquera, A. Pedroza-Tobias, C. Medina, L. Hernandez-Barrera, K. Bibbins-Domingo, R. Lozano, A.E. Moran, Global overview of the epidemiology of atherosclerotic cardiovascular disease, Arch. Med. Res. 46 (2015) 328–338.
[2] T. Inoue, K. Croce, T. Morooka, M. Sakuma, K. Node, D.I. Simon, Vascular inflammation and repair: implications for re-endothelialization, restenosis, and stent thrombosis, JACC, Cardiovascular interventions 4 (2011) 1057–1066.
[3] K.J. Rocha-Singh, M.R. Jaff, T.R. Crabtree, D.A. Bloch, G. Ansel, I. Viva Physicians, Performance goals and endpoint assessments for clinical trials of femoropopliteal bare nitinol stents in patients with symptomatic peripheral arterial disease, Catheter Cardiovasc Interv 69 (2007) 910–919.
[4] P.S. Brookes, Y. Yoon, J.L. Robotham, M.W. Anders, S.S. Sheu, Calcium, ATP, and ROS: a mitochondrial love-hate triangle, Am J Physiol Cell Physiol 287 (2004) C817–C833.

[5] S. Campello, R.A. Lacalle, M. Bettella, S. Manes, L. Scorrano, A. Viola, Orchestration of lymphocyte chemotaxis by mitochondrial dynamics, J. Exp. Med. 203 (2006) 2879–2886.
[6] J. Qing, Z. Zhang, P. Novak, G. Zhao, K. Yin, Mitochondrial metabolism in regulating macrophage polarization: an emerging regulator of metabolic inflammatory diseases, Acta Biochim. Biophys. Sin. 52 (2020) 917–926.
[7] L.W. McQueen, S.S. Ladak, R. Abbasciano, S.J. George, M.S. Suleiman, G. D. Angelini, G.J. Murphy, M. Zakkar, Next-generation and single-cell sequencing approaches to study atherosclerosis and vascular inflammation pathophysiology: a systematic review, Front Cardiovasc Med 9 (2022) 849675.
[8] L. Slenders, D.E. Tessels, S.W. van der Laan, G. Pasterkamp, M. Mokry, The applications of single-cell RNA sequencing in atherosclerotic disease, Front Cardiovasc Med 9 (2022) 826103.
[9] P. Hou, J. Fang, Z. Liu, Y. Shi, M. Agostini, F. Bernassola, P. Bove, E. Candi, V. Rovella, G. Sica, Q. Sun, Y. Wang, M. Scimeca, M. Federici, A. Mauriello, G. Melino, Macrophage polarization and metabolism in atherosclerosis, Cell Death Dis. 14 (2023) 691.
[10] G.J. Koelwyn, E.M. Corr, E. Erbay, K.J. Moore, Regulation of macrophage immunometabolism in atherosclerosis, Nat. Immunol. 19 (2018) 526–537.
[11] M.J. Forteza, D.F.J. Ketelhuth, Metabolism in atherosclerotic plaques: immunoregulatory mechanisms in the arterial wall, Clin. Sci. (Lond.) 136 (2022) 435–454.
[12] A. Singh, D. Faccenda, M. Campanella, Pharmacological advances in mitochondrial therapy, EBioMedicine 65 (2021) 103244.
[13] E.A. Bordt, P. Clerc, B.A. Roelofs, A.J. Saladino, L. Tretter, V. Adam-Vizi, E. Cherok, A. Khalil, N. Yadava, S.X. Ge, T.C. Francis, N.W. Kennedy, L.K. Picton, T. Kumar, S. Uppuluri, A.M. Miller, K. Itoh, M. Karbowski, H. Sesaki, R.B. Hill, B. M. Polster, The putative Drp1 inhibitor mdivi-1 is a reversible mitochondrial complex I inhibitor that modulates reactive oxygen species, Dev. Cell 40 (2017) 583–594.
[14] G. Smith, G. Gallo, To mdivi-1 or not to mdivi-1: is that the question? Dev Neurobiol 77 (2017) 1260–1268.
[15] S.B. Kalkhoran, G.E. Crespo-Avilan, S. Hernandez-Resendiz, C.J.A. Ramachandra, S.G. Ong, D.J. Hausenloy, Pharmacological modulators of mitochondrial dynamics as novel therapeutics for cardiovascular and neurological diseases, Cond. Med. 3 (2020) 16.
[16] A. Daugherty, A.R. Tall, M. Daemen, E. Falk, E.A. Fisher, G. Garcia-Cardena, A. J. Lusis, A.P. Owens, M.E. Rosenfeld 3rd, R. Virmani, T. American Heart association Council on arteriosclerosis, B. Vascular, S. Council on basic cardiovascular, recommendation on Design, execution, and reporting of animal atherosclerosis studies: a scientific statement from the American Heart association, Arterioscler. Thromb. Vasc. Biol. 37 (2017) e131–e157.
[17] D. Schumacher, E.A. Liehn, P. Nilcham, D.C. Mayan, C. Rattanasopa, K. Anand, G. E. Crespo-Avilan, S. Hernandez-Resendiz, R.R. Singaraja, S.A. Cook, D. J. Hausenloy, A neutralizing IL-11 antibody reduces vessel hyperplasia in a mouse carotid artery wire injury model, Sci. Rep. 11 (2021) 20674.
[18] A. Curaj, W. Zhoujun, M. Staudt, E.A. Liehn, Induction of Accelerated Atherosclerosis in Mice: the "Wire-Injury" Model, J Vis Exp, 2020.
[19] E. Shagdarsuren, K. Bidzhekov, Y. Djalali-Talab, E.A. Liehn, M. Hristov, R. A. Matthijsen, W.A. Buurman, A. Zernecke, C. Weber, C1-esterase inhibitor protects against neointima formation after arterial injury in atherosclerosis-prone mice, Circulation 117 (2008) 70–78.
[20] G.K. Yakala, H.A. Cabrera-Fuentes, G.E. Crespo-Avilan, C. Rattanasopa, A. Burlacu, B.L. George, K. Anand, D.C. Mayan, M. Corliano, S. Hernandez-Resendiz, Z. Wu, A. M.K. Schwerk, A.L.J. Tan, L. Trigueros-Motos, R. Chevre, T. Chua, R. Kleemann, E. A. Liehn, D.J. Hausenloy, S. Ghosh, R.R. Singaraja, FURIN inhibition reduces vascular remodeling and atherosclerotic lesion progression in mice, Arterioscler. Thromb. Vasc. Biol. 39 (2019) 387–401.
[21] M. Lopez-Zambrano, J. Rodriguez-Montesinos, G.E. Crespo-Avilan, M. Munoz-Vega, K.T. Preissner, Thrombin promotes macrophage polarization into M1-like phenotype to induce inflammatory responses, Thromb. Haemostasis 120 (2020) 658–670.
[22] M.L. Lopez, G. Bruges, G. Crespo, V. Salazar, P.A. Deglesne, H. Schneider, H. Cabrera-Fuentes, M.L. Schmitz, K.T. Preissner, Thrombin selectively induces transcription of genes in human monocytes involved in inflammation and wound healing, Thromb. Haemostasis 112 (2014) 992–1001.
[23] R. Bzymek, M. Horsthemke, K. Isfort, S. Mohr, K. Tjaden, C. Muller-Tidow, M. Thomann, T. Schwerdtle, M. Bahler, A. Schwab, P.J. Hanley, Real-time two- and three-dimensional imaging of monocyte motility and navigation on planar surfaces and in collagen matrices: roles of Rho, Sci. Rep. 6 (2016) 25016.
[24] C. Kontos, O. El Bounkari, C. Krammer, D. Sinitski, K. Hille, C. Zan, G. Yan, S. Wang, Y. Gao, M. Brandhofer, R.T.A. Megens, A. Hoffmann, J. Pauli, Y. Asare, S. Gerra, P. Bourilhon, L. Leng, H.H. Eckstein, W.E. Kempf, J. Pelisek, O. Gokce, L. Maegdefessel, R. Bucala, M. Dichgans, C. Weber, A. Kapurniotu, J. Bernhagen, Designed CXCR4 mimic acts as a soluble chemokine receptor that blocks atherogenic inflammation by agonist-specific targeting, Nat. Commun. 11 (2020) 5981.
[25] A. Hoffmann, L.C. Zwissler, O. El Bounkari, J. Bernhagen, Studying the pro-migratory effects of MIF, Methods Mol. Biol. 2080 (2020) 1–18.
[26] Y. Zhang, S. Liu, D. Qu, K. Wang, L. Zhang, X. Jing, C. Li, F. Wei, X. Qu, Kif4A mediate the accumulation and reeducation of THP-1 derived macrophages via regulation of CCL2-CCR2 expression in crosstalking with OSCC, Sci. Rep. 7 (2017) 2226.
[27] T.D. Schmittgen, K.J. Livak, Analyzing real-time PCR data by the comparative C(T) method, Nat. Protoc. 3 (2008) 1101–1108.
[28] A.J. Valente, L.A. Maddalena, E.L. Robb, F. Moradi, J.A. Stuart, A simple ImageJ macro tool for analyzing mitochondrial network morphology in mammalian cell culture, Acta Histochem. 119 (2017) 315–326.
[29] M.D. Brand, D.G. Nicholls, Assessing mitochondrial dysfunction in cells, Biochem. J. 435 (2011) 297–312.
[30] M. Keuper, S. Sachs, E. Walheim, L. Berti, B. Raedle, D. Tews, P. Fischer-Posovszky, M. Wabitsch, M. Hrabe de Angelis, G. Kastenmuller, M.H. Tschop, M. Jastroch, H. Staiger, S.M. Hofmann, Activated macrophages control human adipocyte mitochondrial bioenergetics via secreted factors, Mol. Metabol. 6 (2017) 1226–1239.
[31] Y. Liu, R. Xu, H. Gu, E. Zhang, J. Qu, W. Cao, X. Huang, H. Yan, J. He, Z. Cai, Metabolic reprogramming in macrophage responses, Biomark. Res. 9 (2021) 1.
[32] Q. Li, T. Hoppe, Role of amino acid metabolism in mitochondrial homeostasis, Front. Cell Dev. Biol. 11 (2023) 1127618.
[33] R. Umezu, J.I. Koga, T. Matoba, S. Katsuki, L. Wang, N. Hasuzawa, M. Nomura, H. Tsutsui, K. Egashira, Macrophage (Drp1) dynamin-related protein 1 accelerates intimal thickening after vascular injury, Arterioscler. Thromb. Vasc. Biol. 40 (2020) e214–e226.
[34] K. Egashira, Q. Zhao, C. Kataoka, K. Ohtani, M. Usui, I.F. Charo, K. Nishida, S. Inoue, M. Katoh, T. Ichiki, A. Takeshita, Importance of monocyte chemoattractant protein-1 pathway in neointimal hyperplasia after periarterial injury in mice and monkeys, Circ. Res. 90 (2002) 1167–1172.
[35] Y. Asare, J. Koehncke, J. Selle, S. Simsekyilmaz, J. Jankowski, G. Shagdarsuren, J. E. Gessner, J. Bernhagen, E. Shagdarsuren, Differential role for activating FcgammaRIII in neointima formation after arterial injury and diet-induced chronic atherosclerosis in apolipoprotein E-deficient mice, Front. Physiol. 11 (2020) 673.
[36] Y. Shiba, M. Takahashi, T. Yoshioka, N. Yajima, H. Morimoto, A. Izawa, H. Ise, K. Hatake, K. Motoyoshi, U. Ikeda, M-CSF accelerates neointimal formation in the early phase after vascular injury in mice: the critical role of the SDF-1-CXCR4 system, Arterioscler. Thromb. Vasc. Biol. 27 (2007) 283–289.
[37] M.K. Georgakis, J. Bernhagen, L.H. Heitman, C. Weber, M. Dichgans, Targeting the CCL2-CCR2 axis for atheroprotection, Eur. Heart J. 43 (2022) 1799–1808.
[38] A. Schober, C. Weber, Mechanisms of monocyte recruitment in vascular repair after injury, Antioxidants Redox Signal. 7 (2005) 1249–1257.
[39] M.A. Zimmerman, C.H. Selzman, L.L. Reznikov, S.A. Miller, C.D. Raeburn, J. Emmick, X. Meng, A.H. Harken, Lack of TNF-alpha attenuates intimal hyperplasia after mouse carotid artery injury, Am. J. Physiol. Regul. Integr. Comp. Physiol. 283 (2002) R505–R512.
[40] D. Manka, R.G. Collins, K. Ley, A.L. Beaudet, I.J. Sarembock, Absence of p-selectin, but not intercellular adhesion molecule-1, attenuates neointimal growth after arterial injury in apolipoprotein e-deficient mice, Circulation 103 (2001) 1000–1005.
[41] D.R. Manka, P. Wiegman, S. Din, J.M. Sanders, S.A. Green, L.W. Gimple, M. Ragosta, E.R. Powers, K. Ley, I.J. Sarembock, Arterial injury increases expression of inflammatory adhesion molecules in the carotid arteries of apolipoprotein-E-deficient mice, J. Vasc. Res. 36 (1999) 372–378.
[42] S. Oguchi, P. Dimayuga, J. Zhu, K.Y. Chyu, J. Yano, P.K. Shah, J. Nilsson, B. Cercek, Monoclonal antibody against vascular cell adhesion molecule-1 inhibits neointimal formation after periadventitial carotid artery injury in genetically hypercholesterolemic mice, Arterioscler. Thromb. Vasc. Biol. 20 (2000) 1729–1736.
[43] J. Meerschaert, M.B. Furie, The adhesion molecules used by monocytes for migration across endothelium include CD11a/CD18, CD11b/CD18, and VLA-4 on monocytes and ICAM-1, VCAM-1, and other ligands on endothelium, J. Immunol. 154 (1995) 4099–4112.
[44] T. Couffinhal, C. Duplaa, C. Moreau, J.M. Lamaziere, J. Bonnet, Regulation of vascular cell adhesion molecule-1 and intercellular adhesion molecule-1 in human vascular smooth muscle cells, Circ. Res. 74 (1994) 225–234.
[45] R.M. Rao, L. Yang, G. Garcia-Cardena, F.W. Luscinskas, Endothelial-dependent mechanisms of leukocyte recruitment to the vascular wall, Circ. Res. 101 (2007) 234–247.
[46] P.R. Clark, T.D. Manes, J.S. Pober, M.S. Kluger, Increased ICAM-1 expression causes endothelial cell leakiness, cytoskeletal reorganization and junctional alterations, J. Invest. Dermatol. 127 (2007) 762–774.
[47] D. Kesanakurti, C. Chetty, D. Rajasekhar Maddirela, M. Gujrati, J.S. Rao, Essential role of cooperative NF-kappaB and Stat3 recruitment to ICAM-1 intronic consensus elements in the regulation of radiation-induced invasion and migration in glioma, Oncogene 32 (2013) 5144–5155.
[48] A.K. Hubbard, C. Giardina, Regulation of ICAM-1 expression in mouse macrophages, Inflammation 24 (2000) 115–125.
[49] F. Gao, M.B. Reynolds, K.D. Passalacqua, J.Z. Sexton, B.H. Abuaita, M.X. D. O'Riordan, The mitochondrial fission regulator DRP1 controls post-transcriptional regulation of TNF-alpha, Front. Cell. Infect. Microbiol. 10 (2020) 593805.
[50] J.E. Rectenwald, L.L. Moldawer, T.S. Huber, J.M. Seeger, C.K. Ozaki, Direct evidence for cytokine involvement in neointimal hyperplasia, Circulation 102 (2000) 1697–1702.
[51] A. Zernecke, C. Weber, Chemokines in the vascular inflammatory response of atherosclerosis, Cardiovasc. Res. 86 (2010) 192–201.
[52] S.C. Dreskin, G.W. Thomas, S.N. Dale, L.E. Heasley, Isoforms of Jun kinase are differentially expressed and activated in human monocyte/macrophage (THP-1) cells, J. Immunol. 166 (2001) 5646–5653.
[53] K.A. Zarember, P.J. Godowski, Tissue expression of human Toll-like receptors and differential regulation of Toll-like receptor mRNAs in leukocytes in response to microbes, their products, and cytokines, J. Immunol. 168 (2002) 554–561.

[54] I. Smokelin, C. Mizzoni, J. Erndt-Marino, D. Kaplan, I. Georgakoudi, Optical changes in THP-1 macrophage metabolism in response to pro- and anti-inflammatory stimuli reported by label-free two-photon imaging, J. Biomed. Opt. 25 (2020) 1–14.
[55] R. Liu, S.C. Wang, M. Li, X.H. Ma, X.N. Jia, Y. Bu, L. Sun, K.J. Yu, An inhibitor of DRP1 (Mdivi-1) alleviates LPS-induced septic AKI by inhibiting NLRP3 inflammasome activation, BioMed Res. Int. 2020 (2020) 2398420.
[56] Y.H. Li, F. Xu, R. Thome, M.F. Guo, M.L. Sun, G.B. Song, R.L. Li, Z. Chai, B. Ciric, A. M. Rostami, M. Curtis, C.G. Ma, G.X. Zhang, Mdivi-1, a mitochondrial fission inhibitor, modulates T helper cells and suppresses the development of experimental autoimmune encephalomyelitis, J. Neuroinflammation 16 (2019) 149.
[57] S.J. Forrester, K.J. Preston, H.A. Cooper, M.J. Boyer, K.M. Escoto, A.J. Poltronetti, K.J. Elliott, R. Kuroda, M. Miyao, H. Sesaki, T. Akiyama, Y. Kimura, V. Rizzo, R. Scalia, S. Eguchi, Mitochondrial fission mediates endothelial inflammation, Hypertension 76 (2020) 267–276.
[58] X. Liu, X. Zhang, X. Niu, P. Zhang, Q. Wang, X. Xue, G. Song, J. Yu, G. Xi, L. Song, Y. Li, C. Ma, Mdivi-1 Modulates Macrophage/Microglial Polarization in Mice with EAE via the Inhibition of the TLR2/4-GSK3beta-NF-kappaB Inflammatory Signaling Axis, Mol Neurobiol, 2021.
[59] Z.D. Su, C.Q. Li, H.W. Wang, M.M. Zheng, Q.W. Chen, Inhibition of DRP1-dependent mitochondrial fission by Mdivi-1 alleviates atherosclerosis through the modulation of M1 polarization, J. Transl. Med. 21 (2023) 427.
[60] A. Tobler, B. Moser, B. Dewald, T. Geiser, H. Studer, M. Baggiolini, M.F. Fey, Constitutive expression of interleukin-8 and its receptor in human myeloid and lymphoid leukemia, Blood 82 (1993) 2517–2525.
[61] A.A. Baqui, T.F. Meiller, W.A. Falkler, Enhanced interleukin-8 production in THP-1 human monocytic cells by lipopolysaccharide from oral microorganisms and granulocyte-macrophage colony-stimulating factor, Oral Microbiol. Immunol. 14 (1999) 275–280.
[62] I. Corre, D. Pineau, S. Hermouet, Interleukin-8: an autocrine/paracrine growth factor for human hematopoietic progenitors acting in synergy with colony stimulating factor-1 to promote monocyte-macrophage growth and differentiation, Exp. Hematol. 27 (1999) 28–36.
[63] A. Angajala, S. Lim, J.B. Phillips, J.H. Kim, C. Yates, Z. You, M. Tan, Diverse roles of mitochondria in immune responses: novel insights into immuno-metabolism, Front. Immunol. 9 (2018) 1605.
[64] J. Van den Bossche, J. Baardman, M.P. de Winther, Metabolic Characterization of Polarized M1 and M2 Bone Marrow-Derived Macrophages Using Real-Time Extracellular Flux Analysis, J Vis Exp, 2015.
[65] A. Viola, F. Munari, R. Sanchez-Rodriguez, T. Scolaro, A. Castegna, The metabolic signature of macrophage responses, Front. Immunol. 10 (2019) 1462.
[66] M.C. Nelson, R.M. O'Connell, MicroRNAs: at the interface of metabolic pathways and inflammatory responses by macrophages, Front. Immunol. 11 (2020) 1797.
[67] H. Zuo, Y. Wan, Metabolic reprogramming in mitochondria of myeloid cells, Cells (2019) 9.
[68] T. Shirai, R.R. Nazarewicz, B.B. Wallis, R.E. Yanes, R. Watanabe, M. Hilhorst, L. Tian, D.G. Harrison, J.C. Giacomini, T.L. Assimes, J.J. Goronzy, C.M. Weyand, The glycolytic enzyme PKM2 bridges metabolic and inflammatory dysfunction in coronary artery disease, J. Exp. Med. 213 (2016) 337–354.
[69] E. Lachmandas, L. Boutens, J.M. Ratter, A. Hijmans, G.J. Hooiveld, L.A. Joosten, R. J. Rodenburg, J.A. Fransen, R.H. Houtkooper, R. van Crevel, M.G. Netea, R. Stienstra, Microbial stimulation of different Toll-like receptor signalling pathways induces diverse metabolic programmes in human monocytes, Nat Microbiol 2 (2016) 16246.
[70] P.K. Langston, A. Nambu, J. Jung, M. Shibata, H.I. Aksoylar, J. Lei, P. Xu, M. T. Doan, H. Jiang, M.R. MacArthur, X. Gao, Y. Kong, E.T. Chouchani, J. W. Locasale, N.W. Snyder, T. Horng, Glycerol phosphate shuttle enzyme GPD2 regulates macrophage inflammatory responses, Nat. Immunol. 20 (2019) 1186–1195.
[71] W. Dai, G. Wang, J. Chwa, M.E. Oh, T. Abeywardana, Y. Yang, Q.A. Wang, L. Jiang, Mitochondrial division inhibitor (mdivi-1) decreases oxidative metabolism in cancer, Br. J. Cancer 122 (2020) 1288–1297.
[72] S. Courtois, B. de Luxan-Delgado, L. Penin-Peyta, A. Royo-Garcia, B. Parejo-Alonso, P. Jagust, S. Alcala, J.A. Rubiolo, L. Sanchez, B. Sainz Jr., C. Heeschen, P. Sancho, Inhibition of mitochondrial dynamics preferentially targets pancreatic cancer cells with enhanced tumorigenic and invasive potential, Cancers 13 (2021).
[73] C.T. Cheng, C.Y. Kuo, C. Ouyang, C.F. Li, Y. Chung, D.C. Chan, H.J. Kung, D. K. Ann, Metabolic stress-induced phosphorylation of KAP1 Ser473 blocks mitochondrial fusion in breast cancer cells, Cancer Res. 76 (2016) 5006–5018.
[74] Z. Hong, S. Kutty, P.T. Toth, G. Marsboom, J.M. Hammel, C. Chamberlain, J. J. Ryan, H.J. Zhang, W.W. Sharp, E. Morrow, K. Trivedi, E.K. Weir, S.L. Archer, Role of dynamin-related protein 1 (Drp1)-mediated mitochondrial fission in oxygen sensing and constriction of the ductus arteriosus, Circ. Res. 112 (2013) 802–815.
[75] M. Manczak, R. Kandimalla, X. Yin, P.H. Reddy, Mitochondrial division inhibitor 1 reduces dynamin-related protein 1 and mitochondrial fission activity, Hum. Mol. Genet. 28 (2019) 177–199.
[76] M. Picard, O.S. Shirihai, B.J. Gentil, Y. Burelle, Mitochondrial morphology transitions and functions: implications for retrograde signaling? Am. J. Physiol. Regul. Integr. Comp. Physiol. 304 (2013) R393–R406.
[77] M. Buoncervello, S. Maccari, B. Ascione, L. Gambardella, M. Marconi, M. Spada, D. Macchia, T. Stati, M. Patrizio, W. Malorni, P. Matarrese, G. Marano, L. Gabriele, Inflammatory cytokines associated with cancer growth induce mitochondria and cytoskeleton alterations in cardiomyocytes, J. Cell. Physiol. 234 (2019) 20453–20468.
[78] R. Kapetanovic, S.F. Afroz, D. Ramnath, G.M. Lawrence, T. Okada, J.E. Curson, J. de Bruin, D.P. Fairlie, K. Schroder, J.C. St John, A. Blumenthal, M.J. Sweet, Lipopolysaccharide promotes Drp1-dependent mitochondrial fission and associated inflammatory responses in macrophages, Immunol. Cell Biol. 98 (2020) 528–539.
[79] I. Duroux-Richard, C. Roubert, M. Ammari, J. Presumey, J.R. Grun, T. Haupl, A. Grutzkau, C.H. Lecellier, V. Boitez, P. Codogno, J. Escoubet, Y.M. Pers, C. Jorgensen, F. Apparailly, miR-125b controls monocyte adaptation to inflammation through mitochondrial metabolism and dynamics, Blood 128 (2016) 3125–3136.
[80] C. Bogdan, Nitric oxide synthase in innate and adaptive immunity: an update, Trends Immunol. 36 (2015) 161–178.
[81] A. Sica, A. Mantovani, Macrophage plasticity and polarization: in vivo veritas, J. Clin. Invest. 122 (2012) 787–795.
[82] D. Gobelli, P. Serrano-Lorenzo, M.J. Esteban-Amo, J. Serna, M.T. Perez-Garcia, A. Orduna, A.A. Jourdain, M.A. Martin-Casanueva, A.d.l.F. M, M. Simarro, The mitochondrial succinate dehydrogenase complex controls the STAT3-IL-10 pathway in inflammatory macrophages, iScience 26 (2023) 107473.
[83] G.M. Tannahill, A.M. Curtis, J. Adamik, E.M. Palsson-McDermott, A.F. McGettrick, G. Goel, C. Frezza, N.J. Bernard, B. Kelly, N.H. Foley, L. Zheng, A. Gardet, Z. Tong, S.S. Jany, S.C. Corr, M. Haneklaus, B.E. Caffrey, K. Pierce, S. Walmsley, F. C. Beasley, E. Cummins, V. Nizet, M. Whyte, C.T. Taylor, H. Lin, S.L. Masters, E. Gottlieb, V.P. Kelly, C. Clish, P.E. Auron, R.J. Xavier, L.A. O'Neill, Succinate is an inflammatory signal that induces IL-1beta through HIF-1alpha, Nature 496 (2013) 238–242.
[84] L.A.J. O'Neill, M.N. Artyomov, Itaconate: the poster child of metabolic reprogramming in macrophage function, Nat. Rev. Immunol. 19 (2019) 273–281.
[85] E.L. Mills, B. Kelly, A. Logan, A.S.H. Costa, M. Varma, C.E. Bryant, P. Tourlomousis, J.H.M. Dabritz, E. Gottlieb, I. Latorre, S.C. Corr, G. McManus, D. Ryan, H.T. Jacobs, M. Szibor, R.J. Xavier, T. Braun, C. Frezza, M.P. Murphy, L.A. O'Neill, Succinate dehydrogenase supports metabolic repurposing of mitochondria to drive inflammatory macrophages, Cell 167 (2016) 457–470.
[86] A.K. Jha, S.C. Huang, A. Sergushichev, V. Lampropoulou, Y. Ivanova, E. Loginicheva, K. Chmielewski, K.M. Stewart, J. Ashall, B. Everts, E.J. Pearce, E. M. Driggers, M.N. Artyomov, Network integration of parallel metabolic and transcriptional data reveals metabolic modules that regulate macrophage polarization, Immunity 42 (2015) 419–430.
[87] D. Vats, L. Mukundan, J.I. Odegaard, L. Zhang, K.L. Smith, C.R. Morel, R. A. Wagner, D.R. Greaves, P.J. Murray, A. Chawla, Oxidative metabolism and PGC-1beta attenuate macrophage-mediated inflammation, Cell Metabol. 4 (2006) 13–24.
[88] M. Rath, I. Muller, P. Kropf, E.I. Closs, M. Munder, Metabolism via arginase or nitric oxide synthase: two competing arginine pathways in macrophages, Front. Immunol. 5 (2014) 532.
[89] Y. Mao, D. Shi, G. Li, P. Jiang, Citrulline depletion by ASS1 is required for proinflammatory macrophage activation and immune responses, Mol Cell 82 (2022) 527–541.
[90] A.A. Rosdah, B.M. Abbott, C.G. Langendorf, Y. Deng, J.Q. Truong, H.M. M. Waddell, N.X.Y. Ling, W.J. Smiles, L.M.D. Delbridge, G.S. Liu, J.S. Oakhill, S. Y. Lim, J.K. Holien, A novel small molecule inhibitor of human Drp1, Sci. Rep. 12 (2022) 21531.
[91] L.C. Azevedo, M.A. Pedro, L.C. Souza, H.P. de Souza, M. Janiszewski, P.L. da Luz, F.R. Laurindo, Oxidative stress as a signaling mechanism of the vascular response to injury: the redox hypothesis of restenosis, Cardiovasc. Res. 47 (2000) 436–445.
[92] C. Gomez, L. Martinez, A. Mesa, J.C. Duque, L.A. Escobar, S.M. Pham, R.I. Vazquez-Padron, Oxidative stress induces early-onset apoptosis of vascular smooth muscle cells and neointima formation in response to injury, Biosci. Rep. 35 (2015).
[93] K. Hirschberg, T. Radovits, S. Korkmaz, S. Loganathan, S. Zollner, B. Seidel, S. Pali, E. Barnucz, B. Merkely, M. Karck, G. Szabo, Combined superoxide dismutase mimetic and peroxynitrite scavenger protects against neointima formation after endarterectomy in association with decreased proliferation and nitro-oxidative stress, Eur. J. Vasc. Endovasc. Surg. 40 (2010) 168–175.
[94] Y. Zhou, M.J. Zhang, B.H. Li, L. Chen, Y. Pi, Y.W. Yin, C.Y. Long, X. Wang, M. J. Sun, X. Chen, C.Y. Gao, J.C. Li, L.L. Zhang, PPARgamma inhibits VSMC proliferation and migration via attenuating oxidative stress through upregulating UCP2, PLoS One 11 (2016) e0154720.
[95] H. Perlman, L. Maillard, K. Krasinski, K. Walsh, Evidence for the rapid onset of apoptosis in medial smooth muscle cells after balloon injury, Circulation 95 (1997) 981–987.
[96] J. Yin, W. Xia, M. Wu, Y. Zhang, S. Huang, A. Zhang, Z. Jia, Inhibition of mitochondrial complex I activity attenuates neointimal hyperplasia by inhibiting smooth muscle cell proliferation and migration, Chem. Biol. Interact. 304 (2019) 73–82.
[97] H. Bosshart, M. Heinzelmann, THP-1 cells as a model for human monocytes, Ann. Transl. Med. 4 (2016) 438.
[98] D. Wu, A. Dasgupta, K.H. Chen, M. Neuber-Hess, J. Patel, T.E. Hurst, J. D. Mewburn, P.D.A. Lima, E. Alizadeh, A. Martin, M. Wells, V. Snieckus, S. L. Archer, Identification of novel dynamin-related protein 1 (Drp1) GTPase inhibitors: therapeutic potential of Drpitor1 and Drpitor1a in cancer and cardiac ischemia-reperfusion injury, Faseb. J. 34 (2020) 1447–1464.